Synthesis, Molecular Structure, and Nuclear Magnetic Resonance Investigation of the Platinanonaborane and Diplatinadecaborane Cluster Compounds, [4,4-$(PMe_2Ph)_2$-*arachno*-4-PtB_8H_{12}] and [6,6,9,9-$(PMe_2Ph)_4$-*arachno*-6,9-$Pt_2B_8H_{10}$] †

By Simon K. Boocock, Norman N. Greenwood,* Michael J. Hails, John D. Kennedy, and Walter S. McDonald, Department of Inorganic and Structural Chemistry, University of Leeds, Leeds LS2 9JT

The reaction of *cis*-[$PtCl_2(PMe_2Ph)_2$] with an excess of $[B_9H_{14}]^-$ gives 4,4-bis(dimethylphenylphosphine)-*arachno*-4-platinanonaborane, [4,4-$(PMe_2Ph)_2$-4-PtB_8H_{12}], (I), in high yield. The pale yellow crystals are monoclinic, space group $C2/c$, with a = 1.977 1(8), b = 1.302 5(4), c = 1.977 3(4) nm, β = 110.99(3)°, Z = 8, and the molecular structure is that of a nine-vertex *arachno*-platinanonaborane in which the B_8 unit shows trihapto-bonding to the metal centre. The compound is also formed in lower yield from several other polyhedral borane derivatives. The 14-vertex bis(dimethylphenylphosphine)bis-μ-(2—4-η-*nido*-hexaboranyl)-diplatinum(*Pt–Pt*), [$Pt_2(B_6H_9)_2(PMe_2Ph)_2$], is also formed in moderate yield from the $[B_9H_{14}]^-$ reaction, and this offers the most convenient route yet established for its preparation. Treatment of (I) with KH followed by *cis*-[$PtCl_2(PMe_2Ph)_2$] gives the very stable diplatinum compound 6,6,9,9-tetrakis(dimethylphenylphosphine)-*arachno*-6,9-diplatinadecaborane, [6,6,9,9-$(PMe_2Ph)_4$-6,9-$Pt_2B_8H_{10}$], (II). The colourless crystals are monoclinic, space group $C2/c$, with a = 1.376 2(3), b = 1.510 5(4), c = 1.921 0(3) nm, β = 92.59(2)°, and Z = 4; the molecular structure is that of an *arachno*-diplatina-decaborane which features a bis(trihapto) B_8 unit. It is topologically similar to, but not identical with, the *arachno*-decaborane anion $[B_{10}H_{14}]^{2-}$. The ^1H, ^{11}B, ^{31}P, and ^{195}Pt n.m.r. behaviour of both title compounds has been investigated in detail using both single and double resonance techniques, and a number of important structural correlations emerge.

IN recent years there have been a number of synthetic and structural studies in the series of *arachno*-ten-vertex platinum-containing cluster compounds exemplified by [6,6,9-$(PR_3)_3$-6-PtB_9H_{11}],[1] [6,6-$(PMe_3)_2$-6,5,9-$PtC_2B_7H_{11}$],[2] [6,6-$(PPh_3)_2$-6,9-$PtSB_8H_{10}$],[3] [6,6-$(PPh_3)_2$-6,9-$PtCB_8H_{12}$],[4] and [6,6-$(PPh_3)_2$-6,9-$PtNB_8H_{11}$].[5] There has been particular interest in and some dissension concerning the interpretation of these various species in terms of formal cluster electron counts. This prompts us to communicate here definitive results on a further member of this series, the interesting new diplatinadecaborane [6,6,9,9-$(PMe_2Ph)_4$-6,9-$Pt_2B_8H_{10}$], (II), and also on the precursor in its synthesis, the platinanonaborane [4,4-$(PMe_2Ph)_2$-4-PtB_8H_{12}], (I), a compound of known type [1] but for which no structural data have been reported; the location of, and the nature of, the ' pseudo-bridging ' (or ' *endo*-terminal ') *arachno*-hydrogen atoms in this latter compound are of particular theoretical interest.

This work forms part of a wider programme to investigate and interrelate structure, bonding, and important physicochemical characteristics, such as the n.m.r. behaviour, of both mono- and poly-metallaboranes using platinum as a model metal.[6-13] Accordingly we report the results of single-crystal X-ray diffraction analyses and detailed ' multinuclear ' n.m.r. investigations of compounds (I) and (II) together with methods for their syntheses in good yields.

In this paper we use the conventional I.U.P.A.C. recommended [14] numbering systems [structures (1)—(4)] for the constituent atoms of the eleven-, ten-, nine-, and eight-vertex clusters discussed. This has the disadvantage that successive addition of atoms as additional

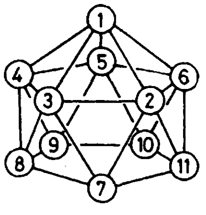

(1a)

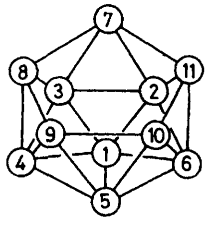

(1b)

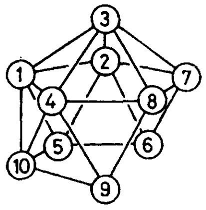

(2a)

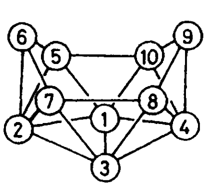

(2b)

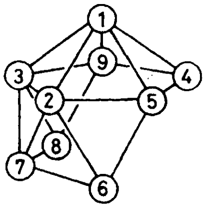

(3a)

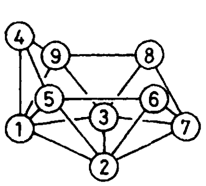

(3b)

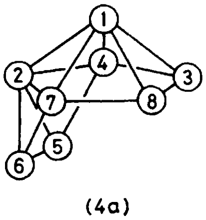

(4a)

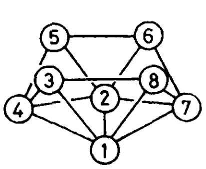

(4b)

---

† 4,4-Bis(dimethylphenylphosphine)-*arachno*-4-platinanonaborane and 6,6,9,9-tetrakis(dimethylphenylphosphine)-*arachno*-6,9-diplatinadecaborane.

vertices to a particular cluster will in general change the numbering of other atoms in the cluster. This may temporarily confuse the reader, but the relationships will be apparent from comparisons among (1a)—(4a) and (1b)—(4b).

RESULTS AND DISCUSSION

I. *Preparation*.—Compounds of the general formula $[L_2PtB_8H_{12}]$, where L is a tertiary phosphine ligand, have been known for some time,[1] and were initially obtained as the products of alcoholic degradation of $[6,6\text{-}L_2\text{-}9\text{-}L'\text{-}6\text{-}PtB_9H_{13}]$ [equation (1)]. We have now

$$[L_2PtB_9H_{13}L'] + 3ROH \longrightarrow [L_2PtB_8H_{12}] + L' + B(OR)_3 + 2H_2 \quad (1)$$

found that $[(PMe_2Ph)_2(PtB_8H_{12})]$ occurs in small but significant amounts in the product mixtures of many reactions, *e.g.* equations (2)—(4),[15,16] but that excellent yields may be obtained by the reaction of *cis*-$[PtCl_2(PMe_2Ph)_2]$ with a two-fold excess of the *arachno*-$[B_9H_{14}]^-$ anion [equation (5)]. This reaction contrasts

$$cis\text{-}[PtCl_2(PMe_2Ph)_2] + 6,6'\text{-}(B_{10}H_{13})_2O \longrightarrow \text{products} \quad (2)$$

$$cis\text{-}[PtCl_2(PMe_2Ph)_2] + B_9H_{13}(SMe_2) + \text{base} \longrightarrow \text{products} \quad (3)$$

$$cis\text{-}[PtCl_2(PMe_2Ph)_2] + B_{10}H_{12}(SMe_2)_2 + \text{base} \longrightarrow \text{products} \quad (4)$$

$$cis\text{-}[PtCl_2(PMe_2Ph)_2] + 2[NMe_4][B_9H_{14}] \longrightarrow [(PMe_2Ph)_2(PtB_8H_{12})]\ (85\%\ \text{yield}) \quad (5)$$

to the other preparations of metallaboranes from $[B_9H_{14}]^-$ that have so far been reported, in which the cluster of nine boron atoms is generally retained in the products. Thus, reaction with $[MnBr(CO)_5]$ resulted in ten-vertex *nido*-metalladecaboranes[17] although low yields of the *arachno*-compound $[(CO)_3(MnB_8H_{13})]$ were also produced;[18] this latter compound however has a completely different structure to those reported here, in that the manganese atom is bonded *via* three Mn–H–B bridge bonds to the 1, 3, and 8 positions [structure (4)] on the neutral B_8H_{13} ligand.[19]

The reaction of $[PtCl_2(PMe_2Ph)_2]$ with $[B_9H_{14}]^-$ also yields a number of other products. Most of these are as yet unidentified, but one is the known[12] 14-vertex binuclear species $[(PMe_2Ph)_4(Pt_2B_{12}H_{18})]$; this is, in fact, obtained in reasonable yield (*ca.* 15%) and this route now provides the most efficient preparative method yet discovered for this interesting compound.

The mechanisms for the formation of these platinum compounds are at present unknown, but the need for an excess of $[B_9H_{14}]^-$ may imply a comproportionation to give also a decaborane species. In any event, $[B_9H_{14}]^-$ is easily made[20] by the base degradation of the readily available *nido*-decaborane, $B_{10}H_{14}$ (we describe a convenient new variant of its synthesis in the Experimental section) and so reaction (5) offers a convenient high-yield synthesis of the very pale yellow crystalline compound $[(PMe_2Ph)_2(PtB_8H_{12})]$. On the basis of their spectroscopic properties compounds of this type have been generally thought[1] to have the nine-vertex *arachno*-4-platina-nonaborane structure: the results of single-crystal *X*-ray diffraction analysis reported below confirm this and provide more precise details of this structural type.

The compound may be regarded as being *formally* derived from the parent *arachno*-octaborane, B_8H_{14},[21] by the replacement of the pair of *endo*-terminal/pseudo-bridging hydrogen atoms in the 3,4 and 4,5 positions [structure (4)] by the neutral $Pt(PMe_2Ph)_2$ moiety (see Discussion, part IV, below). This suggests that the *endo*-terminal hydrogen atoms in the 6,7 and 7,8 positions [structure (3)] in $[(PMe_2Ph)_2(PtB_8H_{12})]$ itself may also be similarly replaceable. This is indeed found to be the case: addition of potassium hydride to $[(PMe_2Ph)_2(PtB_8H_{12})]$ results in the evolution of hydrogen, and subsequent addition of *cis*-$[PtCl_2(PMe_2Ph)_2]$ produces the novel diplatinadecaborane $[(PMe_2Ph)_4(Pt_2B_8H_{10})]$ as an air-stable solid in an isolable pure yield of 55% [equations (6) and (7)]. Interestingly, this is also found as a

$$[(PMe_2Ph)_2(PtB_8H_{12})] + 2KH \longrightarrow [(PMe_2Ph)_2(PtB_8H_{10})]^{2-} + 2K^+ + 2H_2 \quad (6)$$

$$[(PMe_2Ph)_2(PtB_8H_{10})]^{2-} + [PtCl_2(PMe_2Ph)_2] \longrightarrow [(PMe_2Ph)_4(Pt_2B_8H_{10})] + 2Cl^- \quad (7)$$

major product from the treatment of $[(PMe_2Ph)_2(PtB_8H_{12})]$ with alcoholic base. The pure compound is colourless and readily yielded single crystals suitable for *X*-ray diffraction analysis; it appears to be a particularly stable species.

II. *Crystal and Molecular Structures*.—The atomic co-ordinates for 4,4-bis(dimethylphenylphosphine)-*arachno*-4-platinanonaborane, (I), are given in Table 1; selected interatomic distances are in Table 2, and angles between selected interatomic vectors in Table 3. An

TABLE 1

Atomic co-ordinates for (I) with estimated standard deviations in parentheses

	x	*y*	*z*
B(1)	0.058 3(7)	0.093 7(11)	−0.043 9(6)
B(2)	0.118 7(8)	0.028 7(10)	−0.078 3(7)
B(3)	0.079 8(8)	0.149 4(11)	−0.116 5(6)
Pt(4)	0.107 50(2)	0.166 73(3)	0.065 08(2)
B(5)	0.135 4(8)	0.024 0(9)	0.017 0(7)
B(6)	0.209 1(8)	0.031 9(12)	−0.019 8(7)
B(7)	0.172 4(9)	0.125 3(12)	−0.097 4(8)
B(8)	0.140 5(10)	0.256 2(12)	−0.088 1(8)
B(9)	0.070 8(8)	0.231 1(11)	−0.046 3(7)
P(1)	0.139 72(16)	0.089 16(23)	0.177 03(14)
P(2)	0.088 46(16)	0.326 88(24)	0.104 45(15)
C(1)	0.224 1(6)	0.132 0(7)	0.246 5(5)
C(2)	0.232 1(6)	0.135 1(8)	0.320 1(6)
C(3)	0.297 9(7)	0.166 2(10)	0.371 3(6)
C(4)	0.355 1(7)	0.190 8(8)	0.349 4(7)
C(5)	0.347 7(7)	0.189 2(9)	0.276 1(8)
C(6)	0.280 3(6)	0.157 5(9)	0.224 9(6)
C(7)	0.068 4(6)	0.105 2(11)	0.216 6(6)
C(8)	0.152 6(8)	−0.050 3(9)	0.182 3(6)
C(9)	0.149 1(7)	0.368 0(9)	0.195 5(7)
C(10)	0.097 5(7)	0.440 1(9)	0.051 7(7)
C(11)	−0.003 4(6)	0.341 2(9)	0.105 3(5)
C(12)	−0.055 0(7)	0.262 2(10)	0.072 0(6)
C(13)	−0.126 2(7)	0.268 8(12)	0.072 3(7)
C(14)	−0.144 0(8)	0.354 9(13)	0.106 3(8)
C(15)	−0.092 7(9)	0.431 8(12)	0.138 1(8)
C(16)	−0.022 7(8)	0.425 2(10)	0.138 2(7)

TABLE 2

Interatomic distances (pm) for (I) with estimated standard deviations in parentheses

(*i*) From the platinum atom			
Pt(4)–P(1)	230.6(3)	Pt(4)–P(2)	230.4(3)
Pt(4)–B(1)	223.4(12)		
Pt(4)–B(5)	224.5(14)	Pt(4)–B(9)	222.2(13)
(*ii*) Boron–boron			
B(1)–B(2)	179(2)	B(1)–B(3)	179(2)
B(1)–B(5)	181(2)	B(1)–B(9)	181(2)
B(2)–B(3)	179(2)		
B(2)–B(5)	179(2)	B(3)–B(9)	181(2)
B(2)–B(6)	175(2)	B(3)–B(8)	179(2)
B(2)–B(7)	177(2)	B(3)–B(7)	176(2)
B(5)–B(6)	185(2)	B(8)–B(9)	187(3)
B(6)–B(7)	189(2)	B(7)–B(8)	185(2)
(*iii*) Phosphorus–carbon			
P(1)–C(1)	182.8(9)	P(2)–C(9)	184.8(12)
P(1)–C(7)	185.4(14)	P(2)–C(10)	185.1(13)
P(1)–C(8)	183.2(12)	P(2)–C(11)	183.1(13)
(*iv*) Other			
C–C(Ph)	136.6—143.3(18)	mean C–C(Ph)	140.1

TABLE 3

Angles (°) between interatomic vectors for (I) with estimated standard deviations in parentheses

(*i*) At the platinum atom			
P(1)–Pt(4)–P(2)	95.4(1)		
P(1)–Pt(4)–B(1)	127.9(4)	P(2)–Pt(4)–B(1)	130.1(3)
P(1)–Pt(4)–B(5)	91.1(3)	P(2)–Pt(4)–B(9)	87.6(4)
P(1)–Pt(4)–B(9)	175.5(4)	P(2)–Pt(4)–B(5)	170.9(4)
B(1)–Pt(4)–B(5)	47.7(4)	B(1)–Pt(4)–B(9)	47.9(5)
B(5)–Pt(4)–B(9)	86.3(5)		
(*ii*) Platinum–boron–boron			
Pt(4)–B(1)–B(2)	116.8(6)	Pt(4)–B(1)–B(3)	117.1(7)
Pt(4)–B(1)–B(5)	66.5(7)	Pt(4)–B(1)–B(9)	65.7(6)
Pt(4)–B(5)–B(1)	65.8(7)	Pt(4)–B(9)–B(1)	66.4(6)
Pt(4)–B(5)–B(2)	115.9(7)	Pt(4)–B(9)–B(3)	116.9(7)
Pt(4)–B(5)–B(6)	117.9(7)	Pt(4)–B(9)–B(8)	118.2(7)

(*iii*) Boron–boron–boron

(*a*) range 57.0—64.9 mean 60.0
(*b*) range 102.8—116.4 mean 104.0
does not include B(6)–B(7)–B(8) 124.0(10)

(*iv*) Platinum–phosphorus–carbon			
Pt(4)–P(1)–C(1)	116.9(4)	Pt(4)–P(2)–C(9)	117.6(4)
Pt(4)–P(1)–C(7)	111.4(4)	Pt(4)–P(2)–C(10)	118.1(5)
Pt(4)–P(1)–C(8)	118.3(4)	Pt(4)–P(2)–C(11)	112.2(4)

ORTEP drawing of all located atoms is given in Figure 1. The PtB_8 unit is seen to form an open-faced nine-vertex cluster, the six-atom open face and other gross features being similar to those found for nine-vertex *arachno*-nonaborane species such as $B_9H_{13}(NCMe)$ [22] and $[B_9H_{14}]^-$,[23] as distinct from the structures with open faces containing four or five atoms which would be expected for *nido*-nine-vertex species generated by formal removal of an apical or equatorial vertex from the ten-vertex bicapped square-antiprismatic structure represented [24] by $[B_{10}H_{10}]^{2-}$. This confirms the *arachno*-nature of the cluster and the general structural predictions made [1] when this compound type was first reported.

The atomic co-ordinates of the diplatina compound 6,6,9,9-tetrakis(dimethylphenylphosphine)-*arachno*-6,9-diplatinadecaborane, (II), are given in Table 4, selected interatomic distances in Table 5, and selected angles between interatomic vectors in Table 6. An ORTEP drawing to show all atoms of the $Pt_2B_8H_{10}$ cluster is given in Figure 2. The gross structure of the metallaborane unit can be seen to be an open-faced ten-vertex cluster with a six-atom open face, as found in ten-vertex decaborane species with either a *nido*-electron count, as in $B_{10}H_{14}$,[25] or an *arachno*-count, as in $[B_{10}H_{14}]^{2-}$ and $B_{10}H_{12}L_2$.[26,27] In $[(PMe_2Ph)_4(Pt_2B_8H_{10})]$, however, the location of the bridging hydrogen atoms, the magnitudes of the B–B distances, and the n.m.r. properties, as variously discussed below, all indicate an *arachno*-formulation for this compound. It is therefore an analogue of *arachno*-$[B_{10}H_{14}]^{2-}$ in which the BH_2^- groups in the 6 and 9 positions [structure (2)] have been replaced by the isoelectronic [5] (but not exactly isolobal, see below) neutral $Pt(PMe_2Ph)_2$ moieties. This equivalence of BH_2^- and $Pt(PR_3)_2$ appears to be quite general in cluster chemistry, and has ramifications for

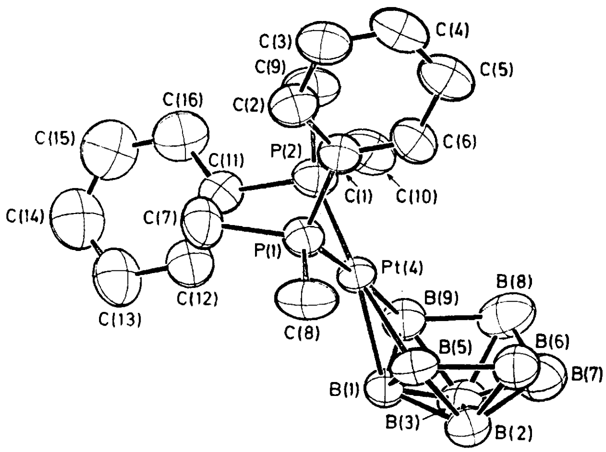

FIGURE 1 ORTEP drawing of the structure of (I). The projection has been chosen to emphasise the structural similarity of the PtB_8 unit to the *arachno*-nonaborane cluster

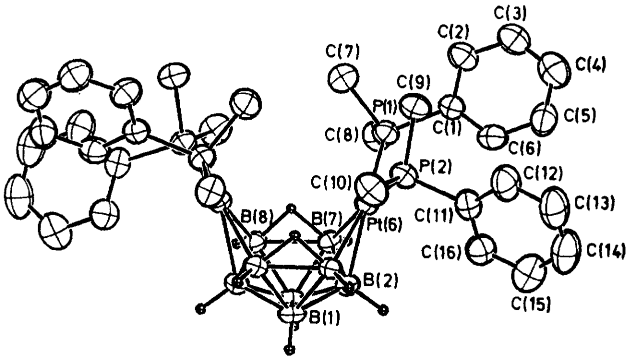

FIGURE 2 ORTEP drawing of the molecular structure of (II). Only the borane hydrogen atoms have been included. The projection has been chosen to emphasise the structural similarity of the Pt_2B_8 unit to the *arachno*-decarboranyl fragment. The molecule has crystallographic symmetry C_2

TABLE 4

Atomic co-ordinates for (II) with estimated standard deviations in parentheses

	x	*y*	*z*
B(1)	−0.061 0(4)	0.441 7(3)	0.234 6(3)
B(2)	0.030 2(4)	0.402 4(3)	0.180 7(3)
Pt(6)	0.039 79(1)	0.259 61(1)	0.158 57(1)
B(7)	0.125 9(4)	0.349 6(3)	0.230 9(3)
B(8)	0.084 0(4)	0.351 9(3)	0.323 5(3)
P(1)	0.165 71(9)	0.158 91(8)	0.164 74(6)
P(2)	−0.061 79(8)	0.183 00(8)	0.081 36(6)
C(1)	0.206 8(3)	0.112 4(3)	0.084 2(2)
C(2)	0.262 8(4)	0.035 3(4)	0.083 7(3)
C(3)	0.297 7(4)	0.005 2(5)	0.022 2(3)
C(4)	0.279 9(4)	0.049 2(4)	−0.038 5(4)
C(5)	0.225 3(5)	0.124 6(4)	−0.038 8(3)
C(6)	0.188 4(4)	0.156 1(4)	0.022 1(3)
C(7)	0.137 0(5)	0.063 3(4)	0.217 0(4)
C(8)	0.281 7(4)	0.190 6(5)	0.206 1(3)
C(9)	−0.044 6(5)	0.064 2(4)	0.071 4(3)
C(10)	−0.192 8(4)	0.183 9(5)	0.092 8(4)
C(11)	−0.053 7(4)	0.226 8(4)	−0.006 5(3)
C(12)	−0.081 7(5)	0.177 3(5)	−0.065 4(3)
C(13)	−0.075 2(5)	0.215 1(6)	−0.131 1(3)
C(14)	−0.042 1(5)	0.297 8(7)	−0.139 2(4)
C(15)	−0.013 4(4)	0.346 9(5)	−0.081 6(4)
C(16)	−0.018 7(4)	0.311 6(4)	−0.015 8(3)
H(1)	−0.097 6(31)	0.496 4(31)	0.228 3(22)
H(2)	0.056 3(31)	0.446 8(34)	0.138 1(24)
H(7)	0.202 1(38)	0.362 7(32)	0.225 7(26)
H(8)	0.141 7(35)	0.369 8(31)	0.363 7(26)
H(78)	0.111 0(33)	0.294 3(37)	0.280 9(24)
H(2)	0.285 0(43)	−0.004 6(43)	0.128 1(32)
H(3)	0.321 9(50)	−0.046 7(49)	0.024 5(34)
H(4)	0.315 6(46)	0.025 9(42)	−0.083 2(33)
H(5)	0.205 6(38)	0.144 9(37)	−0.076 8(30)
H(6)	0.160 0(31)	0.197 3(33)	0.023 4(22)
H(71)	0.095 0(61)	0.009 4(55)	0.193 8(45)
H(72)	0.194 7(49)	0.020 8(45)	0.226 7(32)
H(73)	0.127 3(53)	0.071 9(50)	0.258 8(39)
H(81)	0.323 1(39)	0.144 1(36)	0.207 2(25)
H(82)	0.268 9(36)	0.199 8(39)	0.253 5(31)
H(83)	0.313 9(39)	0.234 5(33)	0.188 6(28)
H(91)	−0.088 2(30)	0.033 5(27)	0.038 5(20)
H(92)	−0.061 5(41)	0.031 3(41)	0.110 6(31)
H(93)	0.018 5(38)	0.051 0(31)	0.071 1(24)
H(101)	−0.220 9(33)	0.152 5(33)	0.051 9(27)
H(102)	−0.220 1(53)	0.142 0(50)	0.144 3(38)
H(103)	−0.216 0(78)	0.221 4(70)	0.105 7(62)
H(12)	−0.108 4(49)	0.112 3(48)	−0.059 6(33)
H(13)	−0.104 1(49)	0.171 1(44)	−0.177 8(38)
H(14)	−0.050 3(61)	0.320 4(57)	−0.190 3(46)
H(15)	0.003 1(47)	0.404 3(44)	−0.085 2(33)
H(16)	−0.006 1(37)	0.350 6(36)	0.023 3(29)

TABLE 5

Interatomic distances (pm) for (II) with estimated standard deviations in parentheses *

(*i*) From the platinum atom			
Pt(6)–P(1)	230.5(1)	Pt(6)–P(2)	230.3(1)
Pt(6)–B(2)	220.3(5)		
Pt(6)–B(5) *	224.1(5)	Pt(6)–B(7)	224.5(5)
(*ii*) Boron–boron			
B(1)–B(2)	176.6(8)	B(1)–B(4) *	176.6(8)
B(1)–B(3) *	175.3(8)		
B(1)–B(5) *	177.6(7)	B(1)–B(10) *	179.5(8)
B(2)–B(5) *	174.5(8)	B(2)–B(7)	178.6(8)
B(7)–B(8)	189.4(8)		
(*iii*) Boron–hydrogen			
B(1)–H(1)	97(5)		
B(2)–H(2)	113(5)		
B(7)–H(7)	108(5)	B(8)–H(8)	112(5)
B(7)–H(78)	130(5)	B(8)–H(78)	126(5)
(*iv*) Phosphorus–carbon			
P(1)–C(1)	181.2(5)	P(2)–C(11)	182.1(5)
P(1)–C(7)	181.3(7)	P(2)–C(9)	182.1(6)
P(1)–C(8)	181.5(6)	P(2)–C(10)	182.7(6)
(*v*) Other			
C–C(Ph)	134—140(1);	mean C–C(Ph)	137.6
C–H	70—124(10);	mean C–H	96

* Due to the C_2 symmetry B(3) is B(1′), B(4) is B(2′), B(5) is B(8′), and B(10) is B(7′).

TABLE 6

Angles (°) between interatomic vectors, with estimated standard deviations in parentheses, for (II)

(*i*) At the platinum atom			
P(1)–Pt(6)–P(2)	97.7(1)		
P(1)–Pt(6)–B(2)	133.5(1)	P(2)–Pt(6)–B(2)	125.2(1)
P(1)–Pt(6)–B(5) *	168.0(1)	P(2)–Pt(6)–B(7)	172.4(1)
P(1)–Pt(6)–B(7)	89.6(1)	P(2)–Pt(6)–B(5) *	88.2(1)
B(2)–Pt(6)–B(5) *	46.2(2)	B(2)–Pt(6)–B(7)	47.3(2)
B(5)–Pt(6)–B(7) *	84.9(2)		
(*ii*) Platinum–boron–boron			
Pt(6)–B(2)–B(1)	119.5(3)	Pt(6)–B(2)–B(3) *	119.5(3)
Pt(6)–B(2)–B(5) *	68.0(3)	Pt(6)–B(2)–B(7)	67.5(3)
Pt(6)–B(5)–B(1) *	117.1(3)	Pt(6)–B(7)–B(3) *	116.1(3)
Pt(6)–B(5)–B(2) *	65.8(3)	Pt(6)–B(7)–B(2)	65.1(3)
Pt(6)–B(5)–B(10) *	113.5(3)	Pt(6)–B(7)–B(8)	114.7(3)
(*iii*) Boron–boron–boron			
B(2)–B(1)–B(3) *	60.2(4)	B(3)–B(1)–B(4) *	60.2(4)
B(2)–B(1)–B(4) *	106.3(4)		
B(2)–B(1)–B(5) *	59.0(3)	B(4)–B(1)–B(10) *	60.2(3)
B(2)–B(1)–B(10) *	109.5(3)	B(4)–B(1)–B(5) *	110.6(3)
B(3)–B(1)–B(5) *	110.7(3)	B(3)–B(1)–B(10) *	111.1(3)
B(5)–B(1)–B(10) *	64.0(3)		
B(1)–B(2)–B(3) *	59.5(4)		
B(1)–B(2)–B(5) *	60.8(4)	B(3)–B(2)–B(7) *	60.7(3)
B(1)–B(2)–B(7)	111.0(4)	B(3)–B(2)–B(5) *	111.5(4)
B(5)–B(2)–B(7) *	118.1(3)		
B(1)–B(5)–B(2) *	60.2(4)	B(1)–B(10)–B(4) *	59.1(3)
B(1)–B(5)–B(10) *	58.5(3)	B(1)–B(10)–B(5) *	57.5(3)
B(2)–B(5)–B(10) *	106.1(3)	B(4)–B(10)–B(5) *	104.6(3)
(*iv*) Platinum–phosphorus–carbon			
Pt(6)–P(1)–C(1)	118.3(1)	Pt(6)–P(2)–C(11)	110.7(2)
Pt(6)–P(1)–C(7)	111.8(2)	Pt(6)–P(2)–C(9)	119.0(2)
Pt(6)–P(1)–C(8)	119.5(2)	Pt(6)–P(2)–C(10)	119.5(2)
(*v*) Selected boron–boron–hydrogen and boron–hydrogen–boron			
B(7)–H(78)–B(8)	96(3)		
B(3)–B(7)–H(78) *	97(2)	B(3)–B(8)–H(78) *	100(2)

* Due to the C_2 symmetry, Pt(9) is Pt(6′), B(3) is B(1′), B(4) is B(2′), B(5) is B(8′), and B(10) is B(7′).

example in the structural interpretations of the so-called ' slipped ' *closo*-metallacarboranes,[28,29] although apparent exceptions are known to occur in small species with particular symmetries, such as in the *closo*-1,6,8-platinadicarbanonaboranes.[30]

Comparison of horizontal rows within each of Tables 2, 3, 5, and 6 shows that there is little deviation from idealised C_s symmetry for the PtB_8 cluster in $[(PMe_2Ph)_2(PtB_8H_{12})]$ and C_{2v} symmetry for the Pt_2B_8 cluster in $[(PMe_2Ph)_4(Pt_2B_8H_{10})]$. The largest deviations from these idealized symmetries occur in the bonds to B(6) and B(8) in the monoplatinum compound. Whether these result from cage electronic effects arising from the different Pt(4)–P(1) and Pt(4)–P(2) bond rotamers or from packing forces is not clear, but in any event the deviations are small.

In each of the two compounds therefore the B_8H_n units can be regarded as ligands which bind to the platinum atoms as symmetrical η^3-B_3 donors, as found[3] for the similar *arachno*-ligand in [6,6-$(PPh_3)_2$-*arachno*-6,9-$PtSB_8H_{10}$], but in contrast to the asymmetric bonding[31] of the η^3-B_3H_7 ligand in [$(PMe_2Ph)_2(PtB_3H_7)$]. It also contrasts with the ' twist ' asymmetry observed[13,16] for the η^4-borane–metal bonding in the 11-vertex [7,7-$(PMe_2Ph)_2$-*nido*-7-$PtB_{10}H_{12}$] and related compounds, but in these the asymmetry arises from crystal packing forces and a low activation energy for ligand pseudorotation about an axis within the platinum bonding plane which is also manifested in intramolecular fluxionality. There is also a twist distortion from ideal symmetry about the platinum atoms in the compounds reported here, presumably also arising from crystal packing forces, but this is small (*ca.* 7° for the monoplatinum and 8.5° for the diplatinum compound), and additionally there is no evidence for rotational fluxionality. The bonding at platinum is therefore rigidly five-co-ordinate to the P(1)P(2)B(1)B(5)B(9) atoms (monoplatinum compound) and the P(1)P(2)B(2)B(5)B(7) atoms (diplatinum compound). Within this co-ordination sphere the formal platinum(II) tetragonal bonding plane for the monoplatinum compound is defined by P(1)P(2)B(5) and B(9) but excludes B(1) [deviation 79 pm from the plane defined by Pt(4)P(1)P(2)], and for the diplatinum compound similarly the tetragonally co-ordinated atoms are P(1)P(2)B(5) and B(7) but B(2) is excluded. The orientation of this formal tetragonal plane is of particular interest, as it differs from that hitherto more generally observed, for example in [$(PMe_2Ph)_2(PtB_3H_7)$][31] and in [5,9-Me_2-6,6-$(PEt_3)_2$-6,5,9-$NiC_2B_7H_9$].[2] For these, the η^3-binding of the metal atom within the cluster is asymmetric in that the formal tetragonal *dsp*^{2} metal bonding plane intersects a B–B vector within the η^3 system and contains only one other cluster atom. This results in a σ,η^2 bidentate cluster binding mode, presumably involving one two-electron two-centre bond and one two-electron three-centre bond. In [$(PMe_2Ph)_2(PtB_8H_{12})$], by contrast {and analogous considerations apply to [$(PMe_2Ph)_4(Pt_2B_8H_{10})$]}, the geometry indicates that the tetragonally disposed platinum *dsp*^{2} valence electrons form two direct two-electron two-centre σ bonds with the B(5) and B(9) atoms. However, it is also apparent that a strong Pt(4)–B(1) interaction is present, which may therefore indicate a (*dsp*^{2} + *d*)-type of platinum electronic involvement with the cluster, as discussed below in section IV. Consistent with this, there is evidence for some square-pyramidal distortion in that the platinum atom is somewhat above the mean P(1)P(2)B(5)B(9) (monoplatinum compound) and P(1)P(2)B(5)B(7) (diplatinum compound) planes (deviations *ca.* 3 pm and 8 pm respectively).

Within this platinum co-ordination sphere the bonds to phosphorus of *ca.* 230.5 pm lie in the centre of ranges typical for this general type of compound (*e.g.* refs. 30—32 and other refs. cited therein), as do the platinum–boron distances of *ca.* 223 pm.[3,30-32] There is no significant difference in the Pt–B distances when the mono-platinum and diplatinum compounds are compared, nor is there between the direct Pt–B contacts within the same compound; there is only a small difference between these and those in the thiaborane analogue [6,6-$(PPh_3)_2$-6,9-$PtSB_{10}H_{10}$][3] in which the Pt(6)–B(2) distance is somewhat shorter [218.4(1.6) pm]. This geometry contrasts with that of the only other trihapto-boron-donor molecule for which data are so far available: this is the σ,η^2 compound [$(PMe_2Ph)_2(PtB_3H_7)$] mentioned above which has a Pt–B σ-bond length of 238(4) pm, with the distances to the boron atoms in the η^2 bond being 213(2) and 218(4) pm.[31]

The closed deltahedral boron–boron distances of 175—180 pm within the clusters are within ranges normal[33] for polyhedral boron clusters. Of those in the open face the B(6)–B(7)/B(7)–B(8) distance of *ca.* 186.5 pm in [$(PMe_2Ph)_2(PtB_8H_{12})$] is similar to that[22] in the nine-vertex *arachno*-compound B_9H_{13}(NCMe), which is probably similarly structured in this part of the molecule (see below), and also to that of the related *arachno*-$[B_9H_{14}]^-$ anion.[23,34] This distance contracts somewhat upon the replacement of the 6- and 8-*endo*-terminal hydrogen atoms by an η^3-co-ordination to the metal centre; the resulting B(2)–B(5) distance [structure (2)] and its equivalents in the two compounds average *ca.* 179 pm, which is significantly less than those of 186(5) and 192(5) pm measured[31] for [$(PMe_2Ph)_2(PtB_3H_7)$]. The contraction of the B–B bond distance on the replacement of a B–H–B bridge by a bond to a metal centre is also found when the η^4 complex [7,7-$(PMe_2Ph)_2$-*nido*-7-$PtB_{10}H_{12}$] is made from $B_{10}H_{14}$ by replacement of the 5,6 and 9,10 bridging hydrogen atoms with the neutral $Pt(PMe_2Ph)_2$ moiety.[16] In the eight-boron clusters described in the present work it is interesting that the contraction is greater for [$(PMe_2Ph)_2(PtB_8H_{12})$] than for the diplatinum compound which may represent a competition in electron demand between the B(3)B(4)B(5) and the B(6)B(7)B(8) η^3-bonding sites of the *arachno*-octaborane nucleus [structure (4)].

The B(5)–B(10)/B(7)–B(8) distances in the ten-vertex system of [$(PMe_2Ph)_4(Pt_2B_8H_{10})$] require particular comment: the distance of 189.4(8) pm is similar to the corresponding ones in the typical *arachno*-species 6,9-$(SMe_2)_2B_{10}H_{12}$ [191(2) pm],[35] 6,9-$(MeCN)_2B_{10}H_{12}$ [188.1(8) pm],[27] [5,9-Me_2-6,6-$(PEt_3)_2$-6,5,9-$NiC_2B_7H_9$] [187(1) pm],[2] and [6,6-$(PPh_3)_2$-6,9-$PtSB_8H_{10}$] [184.4(2.8) pm].[3] It is much shorter than the corresponding distances in typical *nido*-ten-vertex structures such as $B_{10}H_{14}$ [197.3(4) pm][25] and [5-(thf)-6,6,6-$(CO)_3$-6-MnB_9H_{12}] (thf = tetrahydrofuran) [203.7(7) pm][18] which is additional evidence consistent with the *arachno*-description of [$(PMe_2Ph)_4(PtB_8H_{10})$].

This conclusion is further reinforced by the location of the hydrogen atoms in the 5,10 and 7,8 bridging positions in [$(PMe_2Ph)_4(Pt_2B_8H_{10})$]. Data were sufficiently good for these to be reasonably well defined, with a mean $B\text{–}H_{\text{bridge}}$ distance of *ca.* 128 pm (Table 5). Bridging atoms in these positions are characteristic of ten-vertex *arachno*-structures,[2,3,25,27,35] and their incidence is also required for a correct[36] *arachno*-ten-vertex cluster electron count on the assumption that the neutral $Pt(PMe_2Ph)_2$ unit is a BH_2^- subrogator. In accord with this the distance of *ca.* 128 pm is similar to the equivalent distances of *ca.* 125 pm measured by *X*-ray diffraction analysis for $[B_{10}H_{14}]^{2-}$, $L_2B_{10}H_{12}$, *etc.*[25,27,35] In addition to these bridging hydrogens, all the other cluster (terminal) hydrogen atoms for this compound were defined with a mean B–H distance of 107 pm (Table 5).

The *X*-ray diffraction analysis of the structure of the monoplatinum compound $[(PMe_2Ph)_2(PtB_8H_{12})]$ on the other hand was limited by decomposition of the crystals in the *X*-ray beam over the periods required to collect sufficiently accurate data for the location of the hydrogen atoms in the molecule. However, selective ^1H-$\{^{11}B\}$ n.m.r. spectroscopy (section III below) showed that there was a terminal hydrogen atom associated with each boron atom, that there were bridging hydrogen atoms associated principally with the 5,6 and 8,9 positions, and that there were two *endo*-terminal (pseudo-bridging) hydrogen atoms associated principally with B(6) and B(8). Peaks corresponding to all these atoms were apparent in the final difference maps, but the limited accuracy of the data precluded precise location of the interesting *endo*-terminal atoms.

III. *Nuclear Magnetic Resonance Studies.*—We have investigated the n.m.r. behaviour of these compounds in some detail. There are few ways of experimentally assessing the electronic distribution within metallaborane clusters, and it is important to assign n.m.r. parameters for known structures so that theories which attempt to describe these parameters and thence the electronic structures may be developed and tested. Such assignments also enable empirical correlations to be established to aid the structural determination of new species. Within this context, the n.m.r. behaviour of $[4,4\text{-}(PMe_2Ph)_2\text{-}4\text{-}PtB_8H_{12}]$ and of $[6,6,9,9\text{-}(PMe_2Ph)_4\text{-}6,9\text{-}Pt_2B_8H_{10}]$ have a number of interesting and important features.

The ^{11}B and ^1H n.m.r. parameters for the metallaborane cluster of the diplatinum compound $[(PMe_2Ph)_4(Pt_2B_8H_{10})]$ are summarised in Table 7. For this compound, 'satellites' arising from coupling to ^{195}Pt (natural abundance 34%) are apparent for two of the ^{11}B resonances, and the ^{11}B spectra (Figure 3) are readily assigned[11] on the basis of relative intensity and of the values of the coupling constants $^nJ(^{195}Pt–^{11}B)$ for the 2,4 and the 5,7,8,10 positions which are within the range expected[3,11] for $n = 1$. These assignments indicate high shielding for the 1,3 nuclei and low shielding for the 2,4 nuclei as observed in *arachno*-species such as $[B_{10}H_{14}]^{2-}$ [$\delta(^{11}B)$ (1,3) *ca.* −42; (2,4) *ca.* −7 p.p.m.][38,39] and $6,9\text{-}(SEt_2)_2B_{10}H_{12}$ [$\delta(^{11}B)$ (1,3) −38.7; (2,4) −2.9 p.p.m.][39] and in contrast to the shieldings in *nido*-$B_{10}H_{14}$ [$\delta(^{11}B)$ (1,3) +11.3; (2,4) −35.8 p.p.m.][40] and other established related *nido*-ten-vertex structures. This is consistent with the *arachno*-description of the cluster established by the *X*-ray diffraction experiments above.

The ^{11}B resonance positions for $[(PMe_2Ph)_2(PtB_8H_{12})]$ are also readily assigned (Table 8); of the two high-field resonances of relative intensity two, that at highest field is reasonably ascribed to the 1,3 position by comparison with the diplatinum compound and with the parent B_8H_{14},[21] and the other positions follow on the basis of relative intensity and incidence of observable couplings $^1J(^{195}Pt–^{11}B)$; the separate 2 and 9 resonances were differentiated by 'partial relaxation'.[41,42]

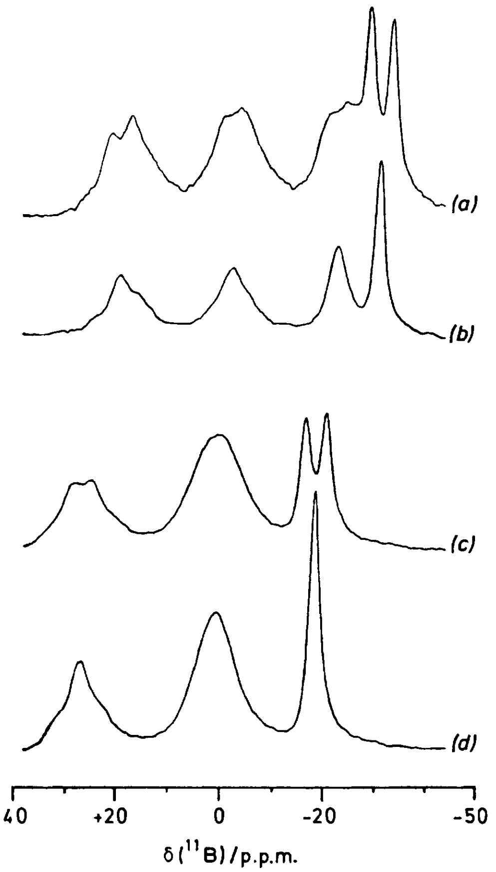

FIGURE 3 32 MHz ^{11}B and ^{11}B-$\{^1H$(broad band)$\}$ n.m.r. spectra of (I) [traces (*a*) and (*b*)] and (II) [traces (*c*) and (*d*)]. Traces (*a*) and (*c*) are normal spectra; (*b*) and (*d*) have $\{^1H$(broad band)$\}$ decoupling. Trace (*a*) has a 2 × increased print-out gain compared to trace (*b*)

As also observed for the eleven-vertex $[7,7\text{-}(PMe_2Ph)_2\text{-}$*nido*$\text{-}7\text{-}PtB_{10}H_{12}]$,[11] the net effect of substitution of platinum on to the octaborane cluster is one of deshielding. The apical positions directly bonded to the metal atom {B(2) and B(4) for $[(PMe_2Ph)_4(Pt_2B_8H_{10})]$; B(1) for $[(PMe_2Ph)_2(PtB_8H_{12})]$} are little affected and the largest deshielding contribution occurs at the platinum-substituted 5,7 and 8,10 positions (diplatinum compound, Table 7) or 5,9 position (monoplatinum compound, Table 8). Interestingly, there is also a large deshielding effect at the apical β positions [B(1,3) in the diplatinum compound, B(2,3) in the monoplatinum compound], an effect again noted[11] for the similar 4 and 6 positions in the eleven-vertex $[(PMe_2Ph)_2(PtB_{10}H_{12})]$.

TABLE 7

Proton and boron-11 n.m.r. data for the borane cluster in (II); saturated solution in CD_2Cl_2 at 21 °C unless otherwise indicated

Assignment	2,4	5,7,8,10	1,3	bridge
$\delta(^{11}B)$/p.p.m.[a]	+28.1	+0.7 [b]	−19.3	
Relative intensity	2	4	2	
SCS(^{11}B)/p.p.m.[c]	−3.2	−21.4	−18.9	
Approx. $T_1(^{11}B)$/ms	1.95	1.23	4.90	
$\delta(^1H)$/p.p.m.[d]	+4.76	+2.94 [e]	+1.57	−1.83
$\delta(^1H)(C_6D_6)$/p.p.m.[d,f]	+6.14	+3.85	[*ca.* +3.5] [g]	−1.28
Relative intensity	2	4	2	2
ASIS(^1H)/p.p.m.[h]	−1.38	−0.91	[−1.9] [g]	−0.55
$^nJ(^{195}Pt-^{11}B)$/Hz	300 ± 40(^1J)	280 ± 60(^1J)	(^2J) [i]	
$^nJ(^{195}Pt-^1H)$/Hz	15 ± 3(^2J)	<*ca.* 15(^2J) [j]	50 ± 5(^3J)	35 ± 5(^2J)
Relative sign	opposite	opposite	not measured	*k*
$^1J(^{11}B-^1H)$/Hz	120 ± 10	110 ± 20	135 ± 10	<*ca.* 70

[a] ±0.5 p.p.m. to high frequency (low field) of $BF_3(OEt_2)$. [b] Possible odd-number multiplet in $^{11}B-\{^1H\}$ spectrum, splitting *ca.* 55 Hz. [c] SCS = ($\delta(B_8H_{14}) - \delta\{[(PMe_2Ph)_4(Pt_2B_8H_{10})]\}$) and is the increase in shielding $\Delta\sigma$ over that measured (ref. 21) for unsubstituted B_8H_{14}. [d] ±0.02 p.p.m. to high frequency (low field) of $SiMe_4$. [e] Partially resolved fine structure apparent in $^1H-\{^{11}B\}$ spectra probably arising principally from $^3J(^{31}P-^1H)$ interactions. [f] Saturated solution in C_6D_6 at 21 °C. [g] Uncertain. [h] ASIS = Aromatic solvent induced shielding (T. Onak, W. Inman, H. Rosendo, E. W. Distefano, and J. Nurse, *J. Am. Chem. Soc.*, 1977, **99**, 6488) = [δ(in CD_2Cl_2) − δ(in C_6D_6)] in this case and is the increase in *shielding* $\Delta\sigma$ on dissolution in the aromatic solvent. [i] ^2J not resolved, *i.e.* $|^2J| <$ *ca.* 90 Hz. [j] The apparent small size of this compared to that for $[(PMe_2Ph)_2(PtB_8H_{12})]$ (Table 8) indicates that $^3J(^{195}Pt-^1H)$ of opposite sign may also be present. [k] $^1H-\{^{11}B\}$ experiments showed differential effects which were not interpretable in terms of the sign being opposite to that of (presumably positive) $^1J[^{195}Pt-^{11}B(5,7,8,10)]$; however, these results were not as definitive as for the 2,4 nuclei which suggests that a negative coupling $^2J[^{195}Pt-^{11}B(5,7,8,10)]$ may also be involved (compare A. G. Davies, M.-W. Tse, J. D. Kennedy, W. McFarlane, M. F. C. Ladd, and D. C. Povey, *J. Chem. Soc., Chem. Commun.*, 1978, 791; J. E. Sarneski, L. E. Erikson, and C. N. Reilly, *J. Magn. Reson.*, 1980, **37**, 155).

TABLE 8

Proton and boron-11 n.m.r. data for the borane cluster in (I); saturated solution in $CDCl_3$ at 21 °C unless otherwise indicated

Assignment	1	7	5,9	6,8	2,3	bridge 5,6 and 8,9	pseudo-bridge 6 and 8
$\delta(^{11}B)$/p.p.m.[a]	+21.6	+18.8	+1.7 [b]	−23.0	−31.6		
Relative intensity	1	1	2	2	2		
SCS(^{11}B)/p.p.m.[c]	+3.3	+6.1	−19.0	+2.3	−6.6		
Approx. $T_1(^{11}B)$/ms	3.2	1.6	1.9	2.0	5.6		
$\delta(^1H)$/p.p.m.[d]	+3.97	+4.20	+2.97 [e]	+2.12	+0.92	−3.05	+0.25
$\delta(^1H)(C_6D_6)$/p.p.m.[d,f]	+4.97	+4.97	+3.53 [e]	+2.88	+2.08	−2.66	+0.81
Relative intensity	1	1	2	2	2	2	2
ASIS(^1H)/p.p.m.[g]	−1.00	−0.77	−0.56	−0.76	−1.16	−0.39	−0.56
$^nJ(^{195}Pt-^{11}B)$/Hz	330 ± 50(^1J)	*h*	260 ± 50(^1J)	*h*	*h*		
$^nJ(^{195}Pt-^1H)$/Hz	<*ca.* 20	*i*	30 ± 5(^2J)	*i*	62 ± 2(^3J)	43 ± 2(^2J)	*i*
Relative sign	not measured [j]	*i*	opposite	*i*	*k*	*k*	*i*
$^1J(^{11}B-^1H)$/Hz	135 ± 5	140 ± 20	140 ± 5	135 ± 5	145 ± 5	<70	<70

[a] See footnote *a* to Table 7. [b] Possible fine structure in ^{11}B spectrum due to $^1J(^{11}B-^1H_{bridge})$ of *ca.* 50 Hz. [c] SCS = ($\delta(B_8H_{14}) - \delta\{[(PMe_2Ph)_2(PtB_8H_{12})]\}$), see footnote *c* to Table 7. [d] See footnote *d* to Table 7. [e] Some fine structure splitting *ca.* 10 Hz apparent, presumably arising from $^3J(^{31}P-^1H)$ and $^3J(^1H-^1H)$ interactions. [f] See footnote *f* to Table 7. [g] ASIS = [δ(in $CDCl_3$) − δ(in C_6D_6)], see footnote *h* to Table 7. [h] Couplings not resolved, *i.e.* ^2J and ^3J <*ca.* 90 Hz. [i] Smaller couplings ^nJ <*ca.* 15 Hz would not be resolved. [j] Partially obscured by $^1H(7)$. [k] No differential satellite sharpening in $^1H-\{^{11}B\}$ experiments.

For both compounds, the magnitudes of any phosphorus couplings $^2J(^{31}P-Pt-^{11}B)$ or $^3J(^{31}P-Pt-B-^{11}B)$ to the cluster boron atoms are expected to be of the order of up to a few tens of Hz,[10,43,] * but none was definitely resolvable although line-narrowing experiments on $^{11}B-\{^1H$(broad band)$\}$ spectra indicated some fine structure in the 5,7,8,10 ^{11}B lines for the diplatinum compound $[(PMe_2Ph)_4(Pt_2B_8H_{10})]$ which may arise from this (Table 7); in any event in this compound the 5,7,8,10 ^{11}B and ^{10}B nuclei and the four ^{31}P nuclei will constitute at simplest an $\{[A]_2[X]_2\}_2$ spin system which will result in a complex spectrum that will be complicated further by the other boron nuclei in the molecule. Similar considerations apply to the interpretation of the non-Lorenzian shapes also apparent particularly for the 5,9 resonance in the monoplatinum compound $[(PMe_2Ph)_2(PtB_8H_{12})]$.

For both compounds, the ^1H n.m.r. resonances of the borane cluster hydrogen atoms were readily observed in $^1H-\{^{11}B\}$ experiments (*e.g.* Figure 4), and selective decoupling experiments [11,42,44,45] assigned their positions and confirmed that each boron atom has a terminal hydrogen atom associated with it (Tables 7 and 8). It was also confirmed for each compound that there are additionally two equivalent bridging hydrogen atoms principally associated with the 5,7,8,10 boron atoms ($Pt_2B_8H_{10}$ compound) and 5,6,8,9 atoms (PtB_8H_{12} compound), again consistent with the solid-state structure and, for $[(PMe_2Ph)_4(Pt_2B_8H_{10})]$ in particular, the *arachno*-description of the cluster bonding. For the monoplatinum compound, the selective decoupling

---

* By comparison with the various couplings involving ^{13}C in organometallic compounds such as *cis*-$[PtMe_2(PMe_2Ph)_2]$ (ref. 43*a*) and $[Pt(CH_2{=}CH_2)(PPh_3)_2]$ (ref. 43*b*).

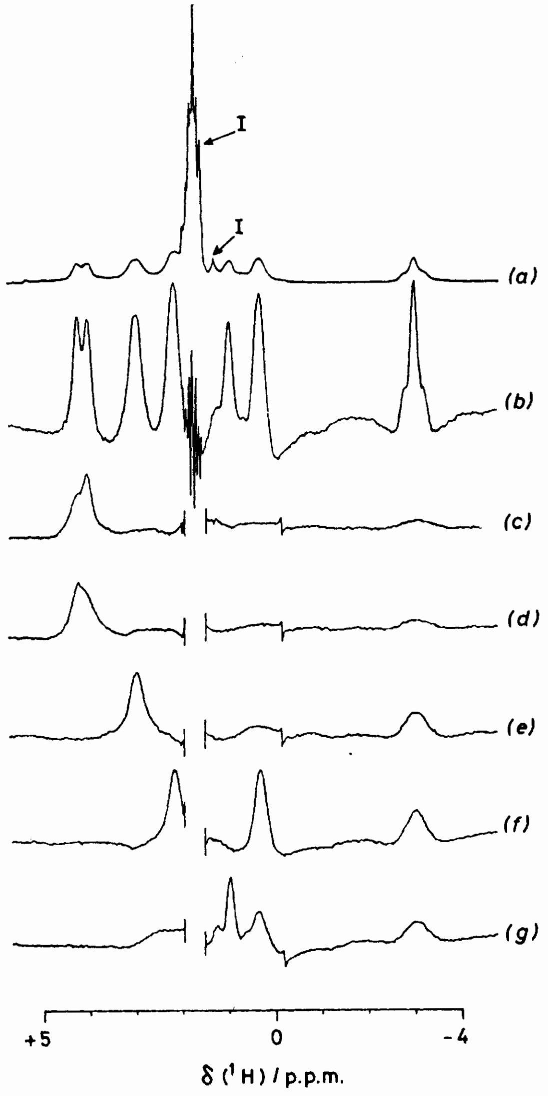

FIGURE 4 100 MHz ^1H-{^{11}B} n.m.r. spectra ($CDCl_3$ solution) of the boron hydride region of (I): (*a*), normal spectrum; (*b*)—(*g*), with the subtraction of equivalent spectra with no {^{11}B} decoupling. Spectra (*a*) and (*b*) have complete {^{11}B(broad band)} decoupling, and (*c*) to (*g*) have selective {^{11}B(CW)} decoupling with $\nu(^{11}B)$ corresponding to $\delta(^{11}B)$ = (*c*) +21.6, (*d*) +18.8, (*e*) −1.7, (*f*) −23.0, and (*g*) −31.6 p.p.m. Peaks I are impurities and the structure centred at $\delta(^1H)$ = *ca.* +1.7 p.p.m. in (*b*) results from the perturbation of the *P*-methyl ^1H resonances upon {^{11}B} irradiation. Note the selective sharpening of the *endo*-terminal resonance at $\delta(^1H)$ = +0.25 p.p.m. upon irradiation at $\nu[^{11}B(6,8)]$ [trace (*f*)] but not upon irradiation at $\nu[^{11}B(7)]$ [trace (*d*)]

experiments also indicated that the *endo*-terminal/pseudo-bridging hydrogen atoms [which resonate at $\delta(^1H)$ = +0.25 p.p.m. ($CDCl_3$ solution) (Table 8)] are associated principally with the 6,8 boron atoms; indeed selective irradiation at $\nu[^{11}B(7)]$ produced no selective sharpening of this proton resonance (Figure 4). This selectivity is similar to that found for the *endo*-terminal protons in the *arachno*-decaboranyl compound 6,9-$(SMe_2)_2B_{10}H_{12}$, $\delta(^1H)$ = −0.37 p.p.m. ($CDCl_3$ solution), which have no bridging character, and are associated with the 6,9 boron resonances only.[16] The *endo*-terminal hydrogens are discussed below in section IV.

The most striking aspect of the measurement and assignment of the proton shieldings of the other (*i.e. exo*) terminal hydrogen atoms for both compounds is the manner in which they parallel the shieldings of the boron atoms to which they are attached (Figure 5). It is notable that the parallel holds also for the boron atoms adjacent to the heavy metal. The line of slope $\delta(^{11}B)/\delta(^1H)$ = 16 is of the same gradient as that observed[42] for a similar plot for the bis(*nido*)-compound 6,6′-$(B_{10}H_{13})_2O$ and indicates that this relationship may be quite general.

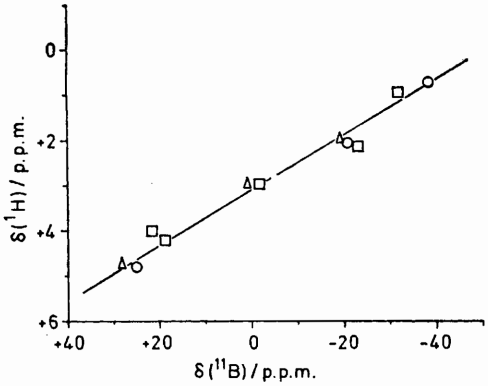

FIGURE 5 Plot of $\delta(^1H)$ against $\delta(^{11}B)$ for the *exo*-terminal B–H groups in B_8H_{14} (○), (I) (□), and (II) (△). Values for the two platinum compounds are from this work ($CDCl_3$ and CD_2Cl_2 solutions respectively), and values for B_8H_{14} (CS_2 and C_5H_{12} solutions) are from ref. 21. The line drawn represents the quotient $\delta(^{11}B)/\delta(^1H)$ = 16

'Satellites' due to coupling with ^{195}Pt were detectable for many of the cluster protons in $[(PMe_2Ph)_2(PtB_8H_{12})]$ and for all of the cluster protons in $[(PMe_2Ph)_4(Pt_2B_8H_{10})]$. For those in terminal positions on boron atoms directly bonded to platinum, selective ^1H-{^{11}B} experiments were used to increase the effective fine-structure resolution in both the ^1H and ^{11}B spectra,[42] and to compare[11] the signs of the corresponding couplings $^1J(^{195}Pt-^{11}B)$ and $^2J(^{195}Pt-^1H)$ (Figure 6 and Tables 7 and 8). In general the values obtained are qualitatively similar to those reported[11] for the $PtB_{10}H_{12}$ cluster in the eleven-vertex compound $[7,7\text{-}(PMe_2Ph)_2\text{-}7\text{-}PtB_{10}H_{12}]$. Firstly, the geminal couplings $^2J(^{195}Pt-B-^1H)$ (bridge or terminal) are smaller (<*ca.* 35 Hz), and the terminal coupling is opposite in sign (where measurable) to the corresponding $^1J(^{195}Pt-^{11}B)$. Secondly, the geometrically similar longer-range vicinal '*trans*-butterfly' couplings $^3J[^{195}Pt-^1H(2,3)]$ (PtB_8H_{12} compound), $^3J[^{195}Pt-^1H(1,3)]$ ($Pt_2B_8H_{10}$ compound), and $^3J[^{195}Pt-^1H(4,6)]$ ($PtB_{10}H_{12}$ compound) [structure (5)] are somewhat larger and are associated with only small couplings $^2J(^{195}Pt-^{11}B)$. We are currently assessing the generality of this and similar emerging patterns of behaviour.

Other selected ^1H, ^{31}P, and ^{195}Pt n.m.r. parameters

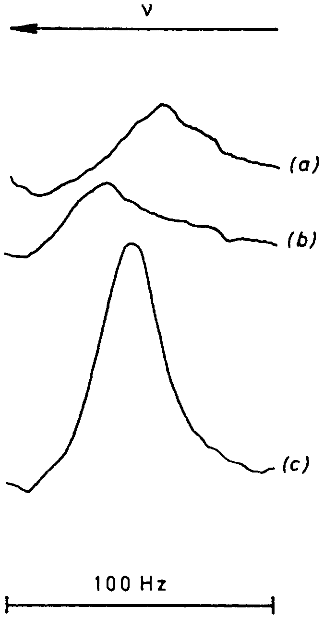

FIGURE 6 100 MHz ^{1}H-{^{11}B} spectra of the 2,4 proton resonance of (II) (CD_2Cl_2 solution) with selective irradiation at (*a*) {$\nu[^{11}B(2,4)] + \frac{1}{2}\,{}^1J(^{195}Pt-^{11}B)$}, (*b*) {$\nu[^{11}B(2,4)] - \frac{1}{2}\,{}^1J(^{195}Pt-^{11}B)$}, and (*c*) $\nu[^{11}B(2,4)]$. These experiments show the presence of $^2J(^{195}Pt-B-^1H)$ = *ca*. 15 Hz and show that its sign is opposite to that of $^1J(^{195}Pt-^{11}B)$

observed for $[(PMe_2Ph)_2(PtB_8H_{12})]$ and $[(PMe_2Ph)_4(Pt_2B_8H_{10})]$ are listed in Table 9 and warrant some comment. In both compounds the phosphine ligands are on prochiral metal centres and the ^{1}H spectra of the *P*-methyl groups consist of two central resonances arising from the consequent inequivalence of the methyl groups,[13,46] flanked by satellite lines arising from coupling to ^{195}Pt; the two slightly different values of $^3J(^{195}Pt-P-C-^1H)$ are as expected.[46] In the absence of {^{31}P} decoupling each resonance resembles the X part of an $[AX_n]_2$ spin system[47] (A = ^{31}P, X = ^{1}H) although the actual spin system which dictates the lineshape will involve the boron nuclei and aromatic protons and be more complex than this. However, the ' *N* lines ' [of separation $N = {}^2J(^{31}P-^1H) + {}^4J(^{31}P-^1H)$ in this case] are common to all these systems and can readily be discerned; the shape[48] of the additional intensity suggests a coupling $|^2J(^{31}P-Pt-^{31}P)|$ somewhat greater than $|N|$, *i.e.* up to a few tens of Hz, consistent with the *cis* stereochemistry at platinum. Selective ^{1}H-{^{31}P} and ^{1}H-{^{195}Pt} experiments[49,50] on the ^{195}Pt satellites of these *P*-methyl resonances confirmed that $^3J(^{195}Pt-^1H)$ is positive and *N* negative relative to $^1J(^{195}Pt-^1H)$ being taken[51] as positive, as again is general[52] in *cis*-bis(phosphine)platinum(II) compounds. As expected from the complex spin system, the *P*-methyl resonances were also affected in ^{1}H-{^{11}B} experiments, but this is not discussed here.

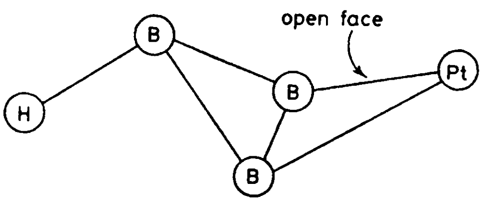

(5)

The ^{31}P-{^{1}H(broad band)} n.m.r. spectrum for each compound (Table 9) consists of a central resonance together with satellites due to ^{195}Pt with $^1J(^{195}Pt-^{31}P)$ *ca*. 2 700 Hz, this value being unexceptional for *cis*-bis(dimethylphenylphosphine)platinum(II) compounds with a bidentate borane(2−) ligand.[10,11,16] At ambient temperatures the resonances are broad due to the effect of adjacent ^{10}B and ^{11}B nuclei, but at lower temperatures these effects become less significant[10] and the lines sharpen.

For the diplatinum compound $[(PMe_2Ph)_4(Pt_2B_8H_{10})]$ this reveals structure arising from small longer-range couplings $^5J(^{31}P-Pt-B-B-Pt-^{31}P)$ and $^4J(^{195}Pt-B-B-Pt-^{31}P)$ (Figure 7). It is apposite to point out here that the origin of this fine structure differs from that observed[9,16] for compounds such as $[4-(2'-B_{10}H_{13})-7,7-(PMe_2Ph)_2-7-PtB_{10}H_{11}]$ which have two chemically inequivalent phosphorus nuclei for which the chemical shifts are accidentally almost degenerate, but for which the different coupling constants $^1J(^{195}Pt-^{31}P)$ give rise to two [AB] sub-spectra at $[\nu(^{31}P)_{mean} \pm \frac{1}{2}\,{}^1J(^{195}Pt-^{31}P)_{mean}]$

TABLE 9

Proton, phosphorus-31, and platinum-195 n.m.r. data for (I) and (II)

Compound	(II)[a]		(I)[b]	
$\delta(^{31}P)$/p.p.m.[c]	-7.7 ± 0.5[d,e]		-6.7 ± 0.5[d]	
$\Xi(^{195}Pt)$/Hz	$21\,383\,640 \pm 200$[f]		$21\,376\,790 \pm 150$[f]	
$^1J(^{195}Pt-^{31}P)$/Hz	$+2\,757 \pm 2$[d]		$+2\,724 \pm 2$[d]	
$^4J(^{195}Pt-^{31}P)$/Hz	-20.8 ± 1.0[d]			
$[^5J(^{31}P-^{31}P)_{cis} + {}^5J(^{31}P-^{31}P)_{trans}]$/Hz[g]	20.0 ± 1.0[d]			
$^3J(^{195}Pt-^{195}Pt)$/Hz	17 ± 8			
$\delta(^1H)$(MeP)/p.p.m.[h,i]	+1.72 (A)	+1.57 (B)	+1.75 (A)	+1.67 (B)
$\delta(^1H)$(MeP)(C_6D_6)/p.p.m.[h,i]	+1.44 (A)	+1.34 (B)	+1.26 (A)	+1.17 (B)
ASIS(^{1}H)/p.p.m.[h,j]	+0.28 (A)	+0.23 (B)	+0.49 (A)	+0.50 (B)
$^3J(^{195}Pt-^1H)$/Hz[h]	$+27.5 \pm 0.5$ (A)	$+23.9 \pm 0.5$ (B)	$+27.3 \pm 0.5$ (A)	$+25.6 \pm 0.5$ (B)
$[^2J(^{31}P-^1H) + {}^4J(^{31}P-^1H)]$/Hz[h]	-8.0 ± 0.5 (A)	-8.0 ± 0.5 (B)	-8.5 ± 0.5 (A)	-8.3 ± 0.5 (B)

[a,b] Saturated solutions in CD_2Cl_2 and $CDCl_3$ at 21 °C respectively unless otherwise indicated. [c] To high frequency of 85% H_3PO_4. [d] At −60 °C. [e] $w_{\frac{1}{2}}$ = 40 Hz (21 °C); 4.5 Hz (−80 °C). [f] Resonances very broad (*cf*. ref. 11). [g] $^5J_{cis}$ and $^5J_{trans}$ probably of same sign and of similar magnitude. [h] (A) and (B) distinguish two inequivalent *P*-methyl groups. [i] To high frequency of $SiMe_4$; ±0.03 p.p.m. [j] See footnote *h* to Table 7.

with splittings arising from the coupling $^{3}J(^{31}P-^{31}P)_{cis}$. In the diplatinadecaborane reported here, by contrast, the observed satellite patterns can be considered as arising in the first instance from an $A[X]_2[X']_2$ spin system (where A = ^{195}Pt, X = ^{31}P) [structure (6)] so that the spectrum (Figure 7) has both 'inner' and 'outer' pairs of satellites at $[\nu(^{31}P) \pm \frac{1}{2}\,^{4}J(^{195}Pt-^{31}P)]$ and $[\nu(^{31}P) \pm \frac{1}{2}\,^{1}J(^{195}Pt-^{31}P)]$ respectively. Each pair of inner and outer satellites constitutes an $[AX]_2$ sub-spectrum[53] (where A and X are here regarded as the two ^{31}P resonance positions for a particular ^{195}Pt spin state) for which the constituent line positions depend upon the three phosphorus–phosphorus couplings $^{2}J(^{31}P-Pt-^{31}P)$, $^{5}J(^{31}P-Pt-B-B-Pt-^{31}P)_{cis}$, and $^{5}J(^{31}P-Pt-B-B-Pt-^{31}P)_{trans}$.

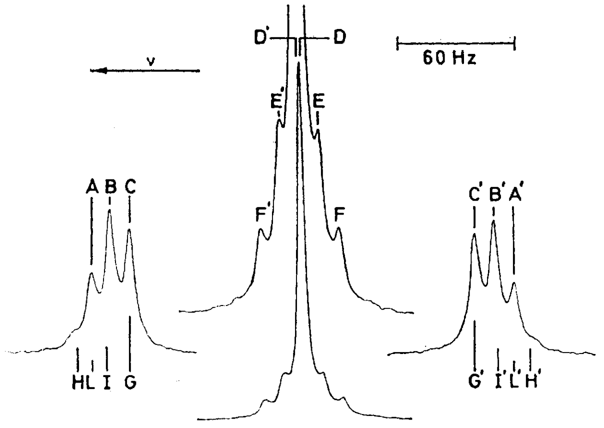

FIGURE 7 40 MHz $^{31}P-\{^{1}H(\text{broad band})\}$ spectra of the central resonance and ^{195}Pt satellites of (II) at −80 °C in CD_2Cl_2 solution. The spectrum is centrosymmetric; lines at A—F arise from species containing one ^{195}Pt nucleus, lines at G—I from species with two ^{195}Pt nuclei: A—C = D—F = $[^{5}J(^{31}P-^{31}P)_{cis} + ^{5}J(^{31}P-^{31}P)_{trans}]$; B—B′ = A—C′ = C—A′ = $^{1}J(^{195}Pt-^{31}P)$; E—E′ = D—F′ = F—D′ = $^{4}J(^{195}Pt-^{31}P)$; and G–G′ = $[^{1}J(^{195}Pt-^{31}P) + ^{4}J(^{195}Pt-^{31}P)]$. Lines at H and I are symmetrically disposed about points L, where L—L′ = L = $[^{1}J(^{195}Pt-^{31}P) - ^{4}J(^{195}Pt-^{31}P)]$; the separation H—I approximates to $^{3}J(^{195}Pt-^{195}Pt)$

Since $^{1}J(^{195}Pt-^{31}P) \gg ^{4}J(^{195}Pt-^{31}P)$ these sub-spectra have negligible second-order character, and the positions of the N lines[53] [where now the separation $N = ^{5}J(^{31}P-^{31}P)_{cis} + ^{5}J(^{31}P-^{31}P)_{trans}$] for both inner and outer satellite systems are readily apparent (Figure 7, lines A, C, D, and F). The rest of the intensity of this spin system is symmetrically disposed about the centre of each N-line pair (*i.e.* at B and E, Figure 7), and the shape of this intensity shows that $|^{5}J(^{31}P-^{31}P)_{cis} - ^{5}J(^{31}P-^{31}P)_{trans}| \ll |^{2}J(^{31}P-^{195}Pt-^{31}P)|$, which implies together with the magnitude of N, that the two longer-range phosphorus–phosphorus couplings have similar magnitudes and signs.

In addition to these transitions, there are also lines arising from the *ca.* 11% of molecules which have *both* metal positions [structure (6)] occupied by ^{195}Pt in natural abundance. In the absence of any residual boron coupling, these will give rise to an $[AX_2]_2$ spin system[54] (A = ^{195}Pt, X = ^{31}P) for which the ^{31}P N lines are at $\nu(^{31}P) \pm \frac{1}{2}N$, where N is now $[^{1}J(^{195}Pt-^{31}P) + ^{4}J(^{195}Pt-^{31}P)]$, and since $^{4}J(^{195}Pt-^{31}P)$ is small these are near the 'outer' satellite patterns arising from molecules with only one ^{195}Pt nucleus. The positions of these lines are also readily apparent (G,G′, Figure 7) and show that $|N| < |^{1}J(^{195}Pt-^{31}P)|$ and therefore that $^{4}J(^{195}Pt-B-B-Pt-^{31}P)$ is negative on the reasonable assumption[51] that $^{1}J(^{195}Pt-^{31}P)$ is positive. The additional intensity (at H, I, Figure 7) from this spin system is symmetrically disposed about each position L (Figure 7), where $L = [^{1}J(^{195}Pt-^{31}P) - ^{4}J(^{195}Pt-^{31}P)]$, with the constituent line positions depending upon $^{3}J(^{195}Pt-^{195}Pt)$ as well as upon the other couplings mentioned above. The spectral resolution obtainable was insufficient for their precise analysis, possibly because of incomplete 'thermal decoupling' of the boron nuclei[10,55] together with more efficient CSA (chemical-shift anisotropy) relaxation[56] of the ^{195}Pt at low temperatures, but it is probable that the separation H–I approximates to $^{3}J(^{195}Pt-^{195}Pt)$ and this indicates a value of *ca.* 17 Hz for this coupling.

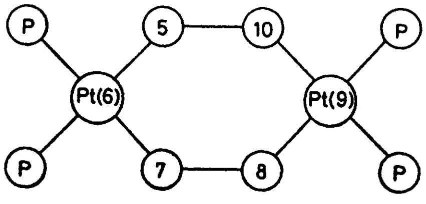

(6)

These results are summarized in Table 9. The observation of the longer-range *trans*-cluster couplings is of interest. Although long-range $^{31}P-^{31}P$, $^{195}Pt-^{31}P$, and $^{195}Pt-^{195}Pt$ couplings are well documented,[57] this is the first time that such long-range couplings *via* several atoms in a polyhedral cluster have been observed. A discussion of the mechanism of their propagation through the cluster must however await more extensive data.

IV. *Structure and Bonding Correlations.*—The compounds $[4,4-(PMe_2Ph)_2-4-PtB_8H_{12}]$, (I), and $[6,6,9,9-(PMe_2Ph)_4-6,9-Pt_2B_8H_{10}]$, (II), can be regarded as covalent platinum(II) complexes of the (hypothetical) *arachno*-$[B_8H_{12}]^{2-}$ and *arachno*-$[B_8H_{10}]^{4-}$ anions respectively. These are conjugate bases of the tetrabasic acid, *arachno*-B_8H_{14}. A consensus of experimental[21,58] and theoretical[59] considerations indicates that this parent compound is non-fluxional with the static structure (7) and that the electronic structure has its basis in structures such as (8) in which the effect of the vacant orbitals on the 4 and 7 boron atoms is mitigated somewhat by partial 'pseudo-bridging' character of the 3, 5, 6, and 8 *endo*-hydrogens (as indicated) together with some additional donation[59] from the electrons in the B(1)–B(2) bond. In structures (7) and (8) each B atom has an *exo*(radial) hydrogen atom in addition to the ones shown. The pseudo-bridging hydrogen atoms are of particular interest, since they resemble the unique pseudo-bridging hydrogen atom[60] in *arachno*-pentaborane, B_5H_{11}. However, in B_5H_{11} dynamic tautomerism of the pseudo-bridging hydrogen atom on B(1) probably occurs [(9) $\rightleftharpoons$ (10), equation (8)] [60] and the precise nature of the interaction has obvious differences to that in B_8H_{14}.

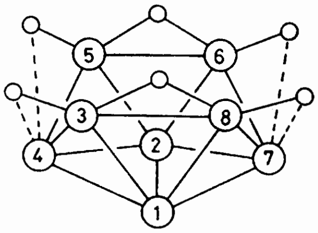

(7)

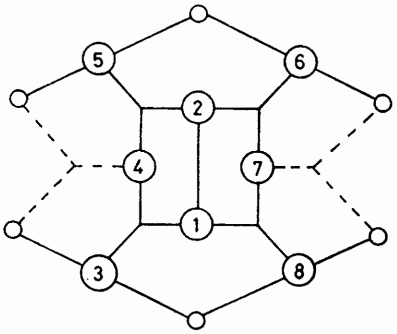

(8)

The determination of the location of the B_8H_{14} pseudo-bridging/*endo*-terminal hydrogen atoms is therefore of interest, but B_8H_{14} itself does not yield crystals suitable for diffraction analysis,[21,58] although *X*-ray data for the *arachno*-nonaborane derivative B_9H_{13}(NCMe),[22] which also has a similar type of hydrogen,[61] indicates that in this case they are in fact *endo*-terminal with no bridging character. It is however important to examine further examples, particularly in the area of eight-boron clusters, and in the present work the n.m.r. properties of the *endo*-terminal hydrogen atoms in [(PMe$_2$Ph)$_2$(PtB$_8$H$_{12}$)] (Table 8) are similar to those in B_8H_{14},[21] and to those in compounds $B_9H_{13}L$,[61] which implies that this pseudo-bridging character is also retained in the platinum compound [schematic structure (11)]. Unfortunately, our samples of [(PMe$_2$Ph)$_2$(PtB$_8$H$_{12}$)] decomposed in the *X*-ray beam in the times required for the collection of data of sufficient quality to locate these atoms accurately, but an indication of their nature arises from the results of selective ^{1}H-{^{11}B} double resonance n.m.r. spectroscopy. The *endo*-hydrogen proton resonance at $\delta = +0.25$ p.p.m. (CDCl$_3$ solution, Table 8) is selectively sharpened by simultaneous irradiation at ν[^{11}B(6,8)] but remains unaffected upon irradiation with similar power levels at ν[^{11}B(7)] (Figure 6). The selectivity is comparable to that found [16] for the *endo*-6,9 terminal protons in *arachno*-6,9-(SMe$_2$)$_2$B$_{10}$H$_{12}$ which have no bridging character. This indicates that in the platinum compound any coupling ^1J[^{11}B(7)–^{1}H(6$_{endo}$ or 8$_{endo}$)] is negligible and consequently that there is little direct *s*-electron overlap between B(7) and the two hydrogen atoms. It also indicates that the low values of the coupling ^1J[^{11}B(6,8)–^{1}H(6,8)$_{endo}$] and the analogous couplings [21,61] in B_8H_{14} and $B_9H_{13}L$ may therefore represent a tendency for the diversion of B(6,8) *p* character into this *endo*-terminal bond and/or a general loss of electron density into the cluster proper. These arguments tend therefore to favour a structure for B_8H_{14} such as in (8), but with minimal hydrogen-atom bridges to the 4 and 7 boron atoms, so that the structure may have substantial contributions from canonical forms having vacant orbitals in these positions.

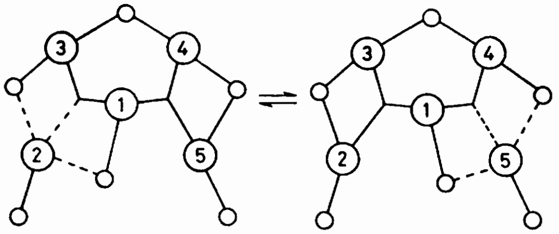

(8)

(9) (10)

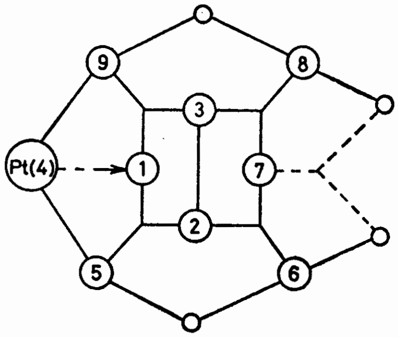

(11)

These considerations have implications in the interpretation of the bonding at platinum in the structures of [(PMe$_2$Ph)$_2$(PtB$_8$H$_{12}$)] and [(PMe$_2$Ph)$_4$(Pt$_2$B$_8$H$_{10}$)]. In these, taking the Pt$_2$B$_8$H$_{10}$ complex as the example, the Pt(6)P(1)P(2)B(5)B(7) system is essentially planar which would be expected if pairs of *endo*-terminal hydrogen atoms with no bridging character were replaced by two direct two-electron two-centre bonds from boron to square-planar platinum(II) [structure (12)]. This structure has many similarities but important differences to that expected on the basis of the supposed [59] electronic structure of the typical *arachno*-decaborane $[B_{10}H_{14}]^{2-}$ [(13); *exo*-hydrogens omitted]. In this, formal subrogation of the 6,9 BH_2^- groups by neutral Pt(PMe$_2$Ph)$_2$ moieties would be expected to yield platinum borane bonds with substantial three-centre character, *i.e.* the platinum(II) square plane of, for example, Pt(6) would intersect the midpoints of the B(2)–B(7) and B(2)–B(5) interatomic vectors, contrary to observation.

The difference arises from the nature of the donation of the extra electron pairs to the cluster bonding. In

$[B_{10}H_{14}]^{2-}$ and related species this is provided by the bonding electron-pairs in the tangential *endo*-terminal B(6)–H(6) and B(9)–H(9) bonds. In $[(PMe_2Ph)_2(PtB_8H_{12})]$ and $[(PMe_2Ph)_4(Pt_2B_8H_{10})]$, however, the Pt–P bonding pairs are *exo*-polyhedral, and the additional cluster electron pairs are therefore supplied by overlap of the tangential occupied platinum (formal) d_{z^2} orbitals with the tangential unoccupied B(1) [structure (11)] or B(2) and B(4) [structure (12)] orbitals, as indicated by the hatched arrows in (11) and (12), and producing a strong bond {*e.g.* Pt(6)–B(2) *ca.* 220 pm in $[(PMe_2Ph)_4(Pt_2B_8H_{10})]$}.

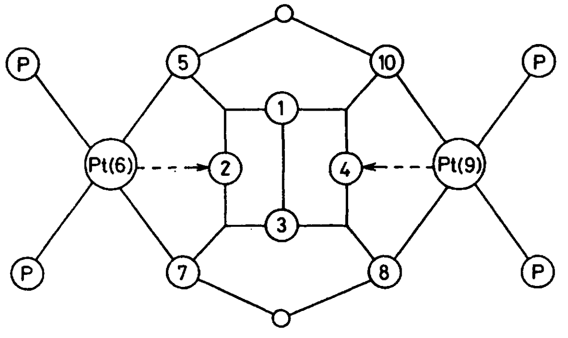

(12)

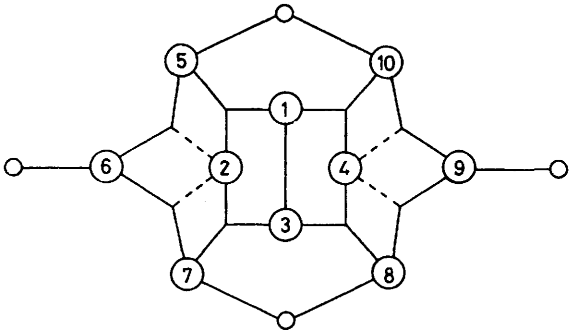

(13)

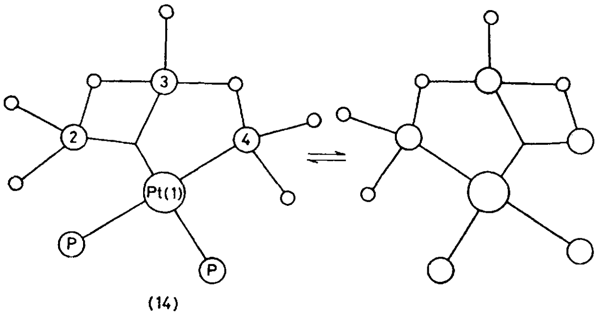

(14)

(9)

The nature of the η^3 interaction in these eight-boron complexes has important differences to that observed for the metallatetraborane [31] $[(PMe_2Ph)_2(PtB_3H_7)]$ and related species,[62] to which parallels with η^3-hydrocarbon ligand interaction have been drawn.[31] Thus, $[(PMe_2Ph)_2(PtB_3H_7)]$ has a η^3 σ,μ-'borallyl' structure in the solid state, (14), but exhibits [16] a mean structure in solution which may be due to the rapid equilibration represented by equation (9) or (less likely) to valence tautomerism when free of crystal packing constraints. In the solid state the platinum(II) square plane of the metallatetraborane accurately contains [31] Pt(1)P(1)P(2)B(4) and the *midpoint* of B(2)–B(3) [structure (14)], and thus clearly involves both a two-electron two-centre and a two-electron three-centre bond, in contrast to the eight-boron species reported here.

In addition, in the metallatetraborane the B–B bonds are much longer,[31] and $^1J[^{195}Pt-^{11}B(3)]$ has the exceptionally large value of 565 ± 10 Hz [16] which also suggests a different type of interaction to that observed for the B_8 species.

EXPERIMENTAL

General.—Reactions were carried out in an atmosphere of dry nitrogen although, except where indicated, no rigorous attention was paid to maintaining anaerobic conditions during the subsequent work-up. Solvents were generally distilled from drying agents under nitrogen before use. The products obtained were reasonably air-stable in the solid state. *nido*-Decaborane was obtained commercially and purified by sublimation before use; *cis*-$[PtCl_2(PMe_2Ph)_2]$ was prepared by standard literature methods; [63] 6,6′-$(B_{10}H_{13})_2O$ was prepared from *arachno*-6,9-$(SMe_2)_2B_{10}H_{12}$ and H_2SO_4; [64] KH was obtained commercially and freed of mineral oil by washing with pentane before use. Thin-layer chromatography (t.l.c.) was carried out on plates made in the laboratory as required from silica gel [Kieselgel 60G (Merck)] and column chromatograms typically used *ca.* 100 g of silica gel [Kieselgel 60 (Merck); 0.063—0.200 mm mesh] in a column of dimensions *ca.* 20 cm × 10 cm². General chromatographic techniques were as described in previous reports from these laboratories.[65,66] Infrared spectra were recorded using KBr discs on a Perkin-Elmer 457 grating instrument, and $\nu_{max.}$ are quoted ± 5 cm^{-1}. Melting points were determined in open capillary tubes.

Preparation of $[NMe_4][B_9H_{14}]$.—The method is an adaptation of that used by Pretzer and Rudolph [67] to generate the anions $[SB_8H_9]^-$ and $[SB_{10}H_{11}]^-$. Potassium hydroxide (0.56 g, 10 mmol) was added to a solution of *nido*-$B_{10}H_{14}$ (1.22 g, 10 mmol) in CH_3OH (20 cm³) and stirred at *ca.* 20 °C for 0.5 h, producing a yellow homogeneous solution with mild effervescence. The solution was allowed to stand overnight, and the liquid components then removed under reduced pressure at $20 < \theta < 40$ °C. Water (15 cm³) was added, the mixture filtered, and a solution of $[NMe_4]Cl$ (6 g, 54 mmol) in water (10 cm³) added. The ***product*** separated as a colourless flocculent precipitate which was filtered off, washed repeatedly with water, and dried *in vacuo* to yield a white powder, $[NMe_4][B_9H_{14}]$ (1.52 g, 8.2 mmol, 82%), identified as such by comparison of n.m.r. and i.r. properties with those [68] in the literature.

Preparation of $[4,4\text{-}(PMe_2Ph)_2\text{-}$*arachno*-$4\text{-}PtB_8H_{12}]$ *from* $[NMe_4][B_9H_{14}]$ *and cis*-$[PtCl_2(PMe_2Ph)_2]$.—The complex *cis*-$[PtCl_2(PMe_2Ph)_2]$ (0.30 g, 0.55 mmol) was dissolved in a solution of $[NMe_4][B_9H_{14}]$ (0.20 g, 1.1 mmol) in CH_2Cl_2 (100 cm³) and allowed to stand overnight. T.l.c. analysis of the very pale yellow solution using CH_2Cl_2–C_6H_{12} (80 : 20) as eluant showed a major product (R_f 0.35) and a minor product (R_f 0.42) as the principal products. The volume was reduced to *ca.* 20 cm^3 under reduced pressure and the resulting mixture was filtered through silica gel [Kieselgel 60 (Merck); mesh 0.063—0.200 mm; *ca.* 5 g], at which point some gas was evolved. The silica gel was repeatedly washed with hot CH_2Cl_2 until the extracts were colourless and did not exhibit the presence of the major component (R_f 0.35) by t.l.c. analysis. The volume of the combined CH_2Cl_2 solutions was reduced to *ca.* 10 cm^3, cyclohexane (*ca.* 10 cm^3) added, and the crude product mixture separated by column chromatography using CH_2Cl_2–C_6H_{12} (50 : 50; *ca.* 1 dm^3) as eluant. The minor yellow product (0.025 g, 0.03 mmol) was identified as bis(dimethylphenylphosphine)bis-μ-(2—4-η-*nido*-hexaboranyl)-diplatinum(*Pt–Pt*), $[Pt_2(\eta^3\text{-}B_6H_9)_2(PMe_2Ph)_2]$, by comparison with an authentic [12] sample. The major component was recrystallised from CH_2Cl_2 (*ca.* 5 cm^3) by slow evaporation under nitrogen, and an additional minor crop was obtained by addition of n-pentane to the mother-liquor followed by cooling to *ca.* −20 °C. This *product*, almost colourless when pure, m.p. (decomp.) 142—144 °C, was identified as 4,4-bis(dimethylphenylphosphine)-*arachno*-4-platinanonaborane, $[4,4\text{-}(PMe_2Ph)_2\text{-}4\text{-}PtB_8H_{12}]$ (total isolated yield 0.275 g, 0.48 mmol, 85%), by comparison with the sample isolated and identified as described below [Found: C, 33.5; H, 6.00; B, 14.8; P, 10.9; Pt (by difference) 34.8. $C_{16}H_{34}B_8P_2Pt$ requires C, 33.7; H, 6.00; B, 15.2; P, 10.9; Pt, 34.2%], $\nu_{max.}$ 2 515 cm^{-1} (ν_{BH}).

Isolation of $[4,4\text{-}(PMe_2Ph)_2\text{-}arachno\text{-}4\text{-}PtB_8H_{12}]$, (I), *from the Reaction of* $6,6'\text{-}(B_{10}H_{13})_2O$ *with cis*-$[PtCl_2(PMe_2Ph)_2]$.—A solution of *cis*-$[PtCl_2(PMe_2Ph)_2]$ (0.21 g, 0.38 mmol) and $6,6'\text{-}(B_{10}H_{13})_2O$ (0.10 g, 0.38 mmol) in CH_2Cl_2–Et_2O (1 : 1, *ca.* 20 cm^3) was stirred at *ca.* 20 °C for 72 h, filtered through silica gel [Kieselgel 60 (Merck), 0.063—0.200 mm mesh; *ca.* 5 g] and washed through with CH_2Cl_2–light petroleum (b.p. 60—80 °C) (50 : 50, *ca.* 100 cm^3). The more volatile components were then removed from the combined filtrates under reduced pressure at $20 < \theta < 60$ °C and the product mixture separated using repeated preparative t.l.c. with CH_2Cl_2–light petroleum (b.p. 60—80 °C) (50 : 50) as eluant, yielding bis(dimethylphenylphosphine)bis-μ-(2—4-η-*nido*-hexaboranyl)-diplatinum(*Pt–Pt*), $[Pt_2(\eta^3\text{-}B_6H_9)_2(PMe_2Ph)_2]$, [12] as one of the products (10 mg, 0.013 mmol, 3.6%), together with somewhat larger quantities of 4,4-bis(dimethylphenylphosphine)-*arachno*-4-platinanonaborane, (I) [R_f 0.35 in CH_2Cl_2–light petroleum (b.p. 60—80 °C) (50 : 50)] (*ca.* 25 mg, 0.044 mmol, 10.5%), which was tentatively identified as such by n.m.r. spectroscopy (Tables 8 and 9). Recrystallisation from hot benzene yielded very pale yellow crystals, m.p. (decomp.) 142—144 °C, of which one was suitable for the *X*-ray diffraction experiments (see below and Tables 1—3, Figure 1) that confirmed the structure.

Preparation of $[6,6,9,9\text{-}(PMe_2Ph)_4\text{-}arachno\text{-}6,9\text{-}Pt_2B_8H_{10}]$, (II).—Potassium hydride (70% active, 0.040 g, corresponding to 0.69 mmol KH) was added to a solution of $[4,4\text{-}(PMe_2Ph)_2\text{-}4\text{-}PtB_8H_{12}]$ (0.15 g, 0.26 mmol) in CH_2Cl_2–thf (66 : 34, 30 cm^3). Mild heating was maintained by use of a hot-air blower and slow effervescence and some darkening of the solution occurred. The complex *cis*-$[PtCl_2(PMe_2Ph)_2]$ (0.143 g, 0.26 mmol) was then added, and the mixture stirred overnight at *ca.* 20 °C, during which time a precipitate developed. T.l.c. analysis of the solution showed one major component (R_f 0.35, 100% CH_2Cl_2 as eluant) together with a small quantity of the starting metallanonaborane (R_f 0.85). The mixture was filtered and the precipitate washed with CH_2Cl_2 until the run-off was colourless. The combined liquids were evaporated to dryness under reduced pressure at $20 < \theta_c < 50$ °C, and the residue separated by column chromatography using CH_2Cl_2 (*ca.* 1 dm^3) as eluant. The major product was recrystallised from CH_2Cl_2 (*ca.* 5 cm^3) by slow evaporation, and an additional minor crop was obtained from the mother-liquor by the addition of n-pentane. The colourless crystalline product, m.p. (decomp.) 194—196 °C, was identified as 6,6,9,9-tetrakis(dimethylphenylphosphine)-*arachno*-6,9-diplatinadecaborane, (II) (0.148 g, 0.14 mmol, 55%), by single-crystal *X*-ray diffraction analysis and n.m.r. spectroscopy as described below and in the text [Found: C, 36.4; H, 5.1; B, 8.0; P, 11.6; Pt (by difference) 38.9. $C_{32}H_{54}B_8P_4Pt_2$ requires C, 37.0; H, 5.25; B, 8.3; P, 11.9; Pt 37.6%], $\nu_{max.}$ 2 500 cm^{-1} (ν_{BH}).

X-*Ray Diffraction Analysis*.—(I). $C_{16}H_{34}B_8P_2Pt$, M = 570.0, Monoclinic, a = 1.977 1(8), b = 1.302 5(4), c = 1.977 3(4) nm, β = 110.99(3)°, U = 4.754(3) nm^3, Z = 8, D_c = 1.593 Mg m^{-3}, $F(000)$ = 2 224, space group $C2/c$, Mo-K_α radiation, graphite monochromatized, λ = 71.069 pm, μ(Mo-K_α) = 6 097 m^{-1}.

(II). $C_{32}H_{54}B_8P_4Pt_2$, M = 1 039.3, Monoclinic, a = 1.376 2(3), b = 1.510 5(4), c = 1.921 0(3) nm, β = 92.59(2)°, U = 3.989(2) nm^3, Z = 4, D_c = 1.731 Mg m^{-3}, $F(000)$ = 2 008, space group $C2/c$, μ(Mo-K_α) = 7 260 m^{-1}.

Structure Determination.—Measurements were made on a Syntex $P2_1$ diffractometer. Cell dimensions and their standard deviations for each compound were obtained by least-squares treatment of the setting angles of 15 reflections having $35 < 2\theta < 40°$. Intensities for all independent reflections with $4 < 2\theta < 50°$ for (I) and with $4 < 2\theta < 45°$ for (II) were measured in the ω—2θ scan mode, with scans running from 1° below α_1 to 1° above α_2. For (II), variable scan speeds (according to a pre-scan intensity) of 1—29° min^{-1} were used. When these scan speeds were used for (I) however, there was substantial decomposition of the crystal during data collection and a much faster data collection with scan speeds of 4—29° min^{-1} was used, when a control reflection showed negligible decline in intensity. In this way 4 331 reflections for (I) and 2 621 for (II) were measured. After correction for Lorentz, polarisation, and transmission factors [A^* = 1.7—3.4 for (I), 2.9—6.7 for (II)] those reflections having $I > 3\sigma(I)$ were retained for the structure analyses [3 194 for (I) and 2 410 for (II)]. The structures were solved from Patterson and electron-density syntheses and full-matrix least-squares refinement with anisotropic temperature factors for non-hydrogen atoms converged at R = 0.042, R' = 0.046 for (I) and R = 0.030, R' = 0.057 for (II). For (II), a difference synthesis then readily gave the hydrogen positions as peaks of 0.43—0.92 e Å^{-3} (430—920 e nm^{-3}). These were included in the refinement, initially as fixed contributions (R = 0.024) and then refined with anisotropic temperature factors, giving a final R of 0.020 and R' = 0.029. For (I), with lower accuracy because of the more rapid data collection, satisfactory hydrogen positions were not obtainable from a difference map, and the structure analysis was terminated at the stage mentioned above. Atomic scattering factors were calculated using the analytical approximation and coefficients given in ref. 69. Least-squares weights were obtained from the modified variances $\sigma^2(I) = \sigma_c^2(I) + (QI)^2$, with Q = 0 for (I) and Q = 0.02 for (II). The final atomic co-ordinates and their estimated standard deviations are given in Tables 1 and 4. Vibration parameters and a list of observed and calculated structure factors are in Supplementary Publication No. SUP 23035 (44 pp.).*

Nuclear Magnetic Resonance Spectroscopy.—100-MHz ^{1}H, ^{1}H-{^{11}B}, and ^{1}H-{^{31}P}, 32-MHz ^{11}B and ^{11}B-{^{1}H}, and 40-MHz ^{31}P-{^{1}H} experiments were carried out on a JEOL FX-100 pulse (Fourier-transform) spectrometer equipped for double resonance. Solutions and conditions were as specified in Tables 7—9 and in the text. Chemical shifts δ are given in p.p.m. to low frequency (' high field ') of $SiMe_4$ for ^{1}H, of $BF_3(OEt_2)$ for ^{11}B, and of 85% H_3PO_4 (Ξ 40 480 730 Hz) for ^{31}P. Boron-11 longitudinal relaxation times $T_1(^{11}B)$ were measured using the π—τ—$\pi/2$ pulse sequence together with the null method; this was calibrated against the semilogarithmic plot method over the range of T_1 values measured using suitable model compounds.[11,42] The π and $\pi/2$ pulses measured for the samples used were found to be 32 and 16 μs respectively. The {X} irradiation power levels used in selective ^{1}H-{X} experiments had previously[11,42] been optimised by trial and error on known compounds for each particular type of decoupling experiment; however, the conditions were not particularly critical. ^{1}H-{^{195}Pt} experiments were carried out at 60 MHz observing frequency in the continuous wave observation mode on a modified JEOL C60-H instrument as described elsewhere.[49]

We thank the S.R.C. for equipment grants, and for a maintenance grant (to M. J. H.), the University of Leeds for a student demonstratorship (to S. K. B.), Mr. A. Hedley for micro-analyses, and Dr. W. McFarlane for collaboration in the ^{1}H-{^{195}Pt} n.m.r. experiments.

[0/1673 *Received*, *3rd November*, 1980]

---

* For details see Notices to Authors No. 7, *J. Chem. Soc., Dalton Trans.*, 1980, Index issue.

REFERENCES

[1] A. R. Kane, L. J. Guggenberger, and E. L. Muetterties, *J. Am. Chem. Soc.*, 1970, **92**, 2571.

[2] M. Green, J. A. K. Howard, K. L. Spencer, and F. G. A. Stone, *J. Chem. Soc., Chem. Commun.*, 1974, 153; *J. Chem. Soc., Dalton Trans.*, 1975, 2274.

[3] D. A. Thompson, T. K. Hilty, and R. W. Rudolph, *J. Am. Chem Soc.*, 1977, **99**, 6774.

[4] G. A. Kukina, I. A. Zakharova, M. A. Porai-Koshic, B. Stíbr, V. G. Sergienko, K. Baše, and J. Dolansky, *Izv. Akad. Nauk SSSR, Ser. Khim.*, 1978, 1229.

[5] K. Baše, A. Petřina, B. Stíbr, V. Petříček, K. Malý, and A. Línek, *Chem. Ind. (London)*, 1979, 212.

[6] N. N. Greenwood, *Pure Appl. Chem.*, 1977, **49**, 791.

[7] N. N. Greenwood, J. D. Kennedy, and J. Staves, *J. Chem. Soc., Dalton Trans.*, 1978, 1146.

[8] J. D. Kennedy, in Proceedings of the 19th International Conference on Coordination Chemistry, Praha, September 1978, vol. 1, p. 79.

[9] S. K. Boocock, N. N. Greenwood, M. J. Hails, J. D. Kennedy, W. S. McDonald, and J. Staves, 4th International Meeting on Boron Chemistry (IMEBORON IV), Salt Lake City, July 1979, paper no. 05.

[10] J. D. Kennedy and J. Staves, *Z. Naturforsch., Teil B*, 1979, **34**, 808.

[11] J. D. Kennedy and B. Wrackmeyer, *J. Magn. Reson.*, 1980, **38**, 529.

[12] N. N. Greenwood, M. J. Hails, J. D. Kennedy, and W. S. McDonald, *J. Chem. Soc., Chem. Commun.*, 1980, 37.

[13] S. K. Boocock, N. N. Greenwood, and J. D. Kennedy, *J. Chem. Soc., Chem. Commun.*, 1980, 307.

[14] R. M. Adams, *Pure Appl. Chem.*, 1972, **30**, 683.

[15] N. N. Greenwood, M. J. Hails, J. D. Kennedy, and W. S. McDonald, unpublished work.

[16] R. Ahmad, Y. M. Cheek, J. E. Crook, N. N. Greenwood, J. D. Kennedy, and W. S. McDonald, unpublished work.

[17] J. W. Lott, D. F. Gaines, H. Shenav, and R. Schaeffer, *J. Am. Chem. Soc.*, 1973, **95**, 3042.

[18] J. W. Lott and D. F. Gaines, *Inorg. Chem.*, 1974, **13**, 2261.

[19] J. C. Calabrese, M. B. Fischer, D. F. Gaines, and J. W. Lott, *J. Am. Chem. Soc.*, 1974, **96**, 6318.

[20] L. E. Benjamin, S. F. Stafiej, and E. A. Takacs, *J. Am. Chem. Soc.*, 1963, **85**, 2674.

[21] D. C. Moody and R. Schaeffer, *Inorg. Chem.*, 1976, **15**, 233.

[22] F. E. Wang, P. G. Simpson, and W. N. Lipscomb, *J. Chem. Phys.*, 1961, **35**, 1335.

[23] N. N. Greenwood, H. J. Gysling, J. A. McGinnety, and J. D. Owen, *Chem. Commun.*, 1970, 505.

[24] R. D. Dobrott and W. N. Lipscomb, *J. Chem. Phys.*, 1962, **37**, 1977.

[25] A. Tippe and W. Hamilton, *Inorg. Chem.*, 1969, **8**, 464.

[26] D. S. Kendall and W. N. Lipscomb, *Inorg. Chem.*, 1973, **12**, 546.

[27] J. Riddy and W. N. Lipscomb, *J. Chem. Phys.*, 1959, **31**, 610; *J. Am. Chem. Soc.*, 1959, **81**, 754.

[28] D. M. P. Mingos, M. I. Forsyth, and A. J. Welch, *J. Chem. Soc., Chem. Commun.*, 1977, 605.

[29] H. M. Colquhoun, T. J. Greenhough, and M. G. H. Wallbridge, *J. Chem. Soc., Chem. Commun.*, 1977, 737; 1978, 322.

[30] M. Green, J. L. Spencer, F. G. A. Stone, and A. J. Welch, *J. Chem. Soc., Chem. Commun.*, 1974, 794.

[31] L. J. Guggenberger, A. R. Kane, and E. L. Muetterties, *J. Am. Chem. Soc.*, 1972, **94**, 5665.

[32] A. J. Welch, *J. Chem. Soc., Dalton Trans.*, 1975, 2270.

[33] N. N. Greenwood, ' Boron,' Pergamon Press, Oxford, 1973, pp. 665—991 and refs. therein.

[34] N. N. Greenwood, J. A. McGinnety, and J. D. Owen, *J. Chem. Soc., Dalton Trans.*, 1972, 986.

[35] D. E. Sands and A. Zalkin, *Acta Crystallogr.*, 1962, **15**, 410.

[36] K. Wade, *Adv. Inorg. Chem. Radiochem.*, 1976, **18**, 1.

[37] L. J. Todd, A. R. Siedle, F. Sato, A. R. Garber, F. R. Scholer, and G. D. Mercer, *Inorg. Chem.*, 1975, **14**, 1249.

[38] E. L. Muetterties, *Inorg. Chem.*, 1963, **2**, 647.

[39] D. E. Hyatt, F. R. Scholer, and L. J. Todd, *Inorg. Chem.*, 1967, **6**, 630.

[40] A. O. Clouse, D. C. Moody, R. R. Rietz, T. Roseberry, and R. Schaeffer, *J. Am. Chem. Soc.*, 1973, **95**, 2496.

[41] A. Allerhand, A. O. Clouse, R. R. Rietz, T. Roseberry, and R. Schaeffer, *J. Am. Chem. Soc.*, 1972, **94**, 2445.

[42] J. D. Kennedy and N. N. Greenwood, *Inorg. Chim. Acta*, 1980, **35**, 93.

[43] (*a*) A. J. Cheney, B. E. Mann, and B. L. Shaw, *Chem. Commun.*, 1971, 431; (*b*) M. H. Chisholm, H. C. Clark, L. E. Manzer, and J. B. Stothers, *J. Am. Chem. Soc.*, 1972, **94**, 5087.

[44] V. T. Aftandalian, H. C. Miller, G. W. Parshall, and E. L. Muetterties, *Inorg. Chem.*, 1962, **1**, 734.

[45] S. K. Boocock, N. N. Greenwood, J. D. Kennedy, and D. Taylorson, *J. Chem. Soc., Chem. Commun.*, 1979, 16.

[46] P. Haake and P. C. Turley, *J. Am. Chem. Soc.*, 1967, **89**, 4611.

[47] R. K. Harris, *Can. J. Chem.*, 1964, **42**, 2275.

[48] E. G. Finer and R. K. Harris, *Mol. Phys.*, 1967, **12**, 457.

[49] J. D. Kennedy, W. McFarlane, R. J. Puddephatt, and P. J. Thompson, *J. Chem. Soc., Dalton Trans.*, 1976, 874.

[50] J. D. Kennedy, W. McFarlane, and R. J. Puddephatt, *J. Chem. Soc., Dalton Trans.*, 1976, 745.

[51] W. McFarlane, *J. Chem. Soc. A*, 1967, 1922.

[52] J. D. Kennedy, I. J. Colquhoun, W. McFarlane, and R. J. Puddephatt, *J. Organomet. Chem.*, 1979, **172**, 479, and refs. therein.

[53] J. Emsley, J. Feeney, and L. Sutcliffe, ' High Resolution NMR Spectroscopy,' Pergamon Press, Oxford, 1966, vol. 1, pp. 392—399.

[54] R. K. Harris, J. R. Wolpin, R. E. Dunmur, M. Murray, and R. Schmutzler, *Ber. Bunsenges. Phys. Chem.*, 1972, **76**, 44.

[55] D. W. Lowman, P. D. Ellis, and J. D. Odom, *J. Magn. Reson.*, 1972, **8**, 289.

[56] J.-Y. Lallemand, J. Soulié, and J.-C. Chottard, *J. Chem. Soc., Chem. Commun.*, 1980, 436.

[57] L. Ernst, *Org. Magn. Reson.*, 1977, **9**, 35; *J. Chem. Soc., Chem. Commun.*, 1977, 375.

[58] J. Dobson and R. Schaeffer, *Inorg. Chem.*, 1968, **7**, 402.

[59] W. N. Lipscomb, *Pure Appl. Chem.*, 1977, **49**, 701.

[60] R. R. Rietz, R. Schaeffer, and L. G. Sneddon, *J. Am. Chem. Soc.*, 1970, **92**, 3514.

[61] R. Schaeffer and E. Walter, *Inorg. Chem.*, 1973, **12**, 2209.

[62] N. N. Greenwood, J. D. Kennedy, and D. Reed, *J. Chem. Soc., Dalton Trans.*, 1980, 196.

[63] See, for example, *Inorg. Synth.*, 1970, **12**, 27.

[64] J. Plešek, S. Heřmánek, and B. Stíbr, *Collect. Czech. Chem. Commun.*, 1967, **32**, 1095.

[65] N. N. Greenwood, J. D. Kennedy, T. R. Spalding, and D. Taylorson, *J. Chem. Soc., Dalton Trans.*, 1979, 840.

[66] S. K. Boocock, N. N. Greenwood, J. D. Kennedy, W. S. McDonald, and J. Staves, *J. Chem. Soc., Dalton Trans.*, 1980, 790.

[67] W. R. Pretzer and R. W. Rudolph, *J. Am. Chem. Soc.*, 1976, **98**, 1441.

[68] R. Schaeffer and L. G. Sneddon, *Inorg. Chem.*, 1972, **11**, 3102; L. E. Benjamin, D. A. Carvalho, S. E. Stafiej, and E. A. Takacs, *Inorg. Chem.*, 1970, **9**, 1844; V. T. Brice, H. D. Johnson, D. L. Denton, and S. G. Shore, *Inorg. Chem.*, 1972, **11**, 1135.

[69] ' International Tables for *X*-Ray Crystallography,' Kynoch Press, Birmingham, 1974, vol. 4.